DOI: 10.1021/om901065g

ORGANOMETALLICS
Article

Carbon−Fluorine Bond Activation in Thermolysis Reactions of the Osmium(IV) Perfluorothiolate Compounds $[Os(SC_6F_5)_4(P(C_6H_4X\text{-}4)_3)]$ (X = CF_3, Cl, F, H, CH_3, and OCH_3)

Consuelo Mendoza,[†] Sylvain Bernès,[‡] Hugo Torrens,[§] and Maribel Arroyo*,[†]

[†]*Centro de Química, Instituto de Ciencias, BUAP, Ciudad Universitaria, San Manuel, 72570 Puebla, Puebla, Mexico,* [‡]*DEP, Facultad de Ciencias Químicas, UANL, Guerrero y Progreso S/N, Col. Treviño 64570 Monterrey, Nuevo León, Mexico, and* [§]*DEP, Facultad de Química, UNAM, Ciudad Universitaria, 04510 México D.F., Mexico*

Received December 11, 2009

Thermolysis reactions of $[Os(SC_6F_5)_4(P(C_6H_4X\text{-}4)_3)]$ (X = CF_3 **1**, Cl **2**, F **3**, H **4**, CH_3 **5**, and OCH_3 **6**) in refluxing toluene yield compounds $[OsF(SC_6F_5)_2(SC_6F_4(SC_6F_5)\text{-}2)(P(C_6H_4X\text{-}4)_3)]$ (**1a**−**6a**) and $[Os(SC_6F_5)_2(SC_6F_4(SC_6F_5)\text{-}2)(C_6H_4X\text{-}4)]$ (**1b**−**6b**). In addition, $[Os(SC_6F_5)_3(SC_6F_4(SC_6F_5)\text{-}2)]$ (**c**) is yielded from **1**−**4** and **6**, compounds $[OsF(SC_6F_5)_3(P(C_6H_4X\text{-}4)_3)]$ [X = CF_3 (**1e**), X = Cl (**2e**)] are also identified as products of the thermolysis reactions of **1** and **2**, while $[Os(SC_6F_5)_2(S_2C_6F_4)(P(C_6H_4CH_3\text{-}4)_3)]$ (**5d**) is obtained from **5**. Compounds **c**, **e**, and **d** are produced in low yields (ca. 2−4%). Formation of all products involves the rupture of *ortho* C−F bonds. The first complexes systematically detected in these thermolysis reactions are compounds **a**, which are isomers of the starting complexes. Thus, the C−F activation involves the metal-mediated generation of the covalent Os−F bond. Single-crystal X-ray diffraction studies of the new compounds **4a**, **5a**, **2b**−**6b**, **2e**, and **5d** indicate that these compounds consist of five-coordinated metal ions in essentially trigonal-bipyramidal geometries. In addition, thermolysis of the isolated compound $[OsF(SC_6F_5)_2(SC_6F_4(SC_6F_5)\text{-}2)(P(C_6H_4CH_3\text{-}4)_3)]$ (**5a**) in refluxing toluene gives rise to $[Os(SC_6F_5)_2(SC_6F_4(SC_6F_5)\text{-}2)(C_6H_4CH_3\text{-}4)]$ (**5b**) and $[Os(SC_6F_5)_2(S_2C_6F_4)(P(C_6H_4CH_3\text{-}4)_3)]$ (**5d**), confirming that compounds **a** can generate compounds **b** when the thermolysis is prolonged. Compounds **1a**−**6a**, **2b**−**6b**, **1e**, and **2e** are investigated in solution by NMR studies, including variable-temperature ^{19}F NMR experiments. These molecules are fluxional. Some of the activation parameters for the dynamic processes are determined.

Introduction

Developments in metal-mediated C−F bond activation have been reviewed,[1] and relevant recent advances have been attained.[2−22] Catalytic or stoichiometric C−F bond functionalization, where a fluorine atom in an organic molecule is replaced by a new group through a metal-mediated reaction, has been reported for the conversion of C−F bonds to C−H bonds (hydrodefluorinations),[4,13,22−24]

*Corresponding author. E-mail: slarroyo@siu.buap.mx.

(1) (a) Perutz, R. N.; Braun, T. In *Comprehensive Organometallic Chemistry III*; Crabtree, R. H., Mingos, D. M. P., Eds.; Elsevier: Oxford, 2007; vol. *1*, pp 725−758. (b) Torrens, H. *Coord. Chem. Rev*. **2005**, *249*, 1957–1985. (c) Jones, W. D. *Dalton Trans*. **2003**, 3991–3995. (d) Mazurek, U.; Schwarz, H. *Chem. Commun*. **2003**, 1321–1326. (e) Braun, T.; Perutz, R. N. *Chem. Commun*. **2002**, 2749–2757. (f) Richmond, T. G. *Angew. Chem., Int. Ed*. **2000**, *39*, 3241–3244. (g) Richmond, T. G. *Topics in Organometallic Chemistry*; Murai, S., Ed.; Springer: New York, 1999; Vol. *3*, pp 243−269. (h) Burdeniuc, J.; Jedlicka, B.; Crabtree, R. H. *Chem. Ber*. **1997**, *130*, 145–154. (i) Saunders, G. C. *Angew. Chem., Int. Ed. Engl*. **1996**, *35*, 2615–2617. (j) Kiplinger, J. L.; Richmond, T. G.; Osterberg, C. E. *Chem. Rev*. **1994**, *94*, 373–431.

(2) Braun, T.; Salomon, M. A.; Altenhöner, K.; Teltewskoi, M.; Hinze, S. *Angew. Chem., Int. Ed*. **2009**, *48*, 1818–1822.

(3) Schwartsburd, L.; Cohen, R.; Konstantinovski, L.; Milstein, D. *Angew. Chem., Int. Ed*. **2008**, *47*, 3603–3606.

(4) Johnson, S. A.; Huff, C. W.; Mustafa, F.; Saliba, M. *J. Am. Chem. Soc*. **2008**, *130*, 17278–17280.

(5) Schaub, T.; Fischer, P.; Steffen, A.; Braun, T.; Radius, U.; Mix, A. *J. Am. Chem. Soc*. **2008**, *130*, 9304–9317.

(6) Wang, T.; Love, J. A. *Organometallics* **2008**, *27*, 3290–3296.

(7) Arisawa, M.; Suzuki, T.; Ishikawa, T.; Yamaguchi, M. *J. Am. Chem. Soc*. **2008**, *130*, 12214–12215.

(8) Wang, T.; Alfonso, B. J.; Love, J. A. *Org. Lett*. **2007**, *9*, 5629–5631.

(9) Lindup, R. J.; Marder, T. B.; Perutz, R. N.; Whitwood, A. C. *Chem. Commun*. **2007**, 3664–3666.

(10) Cole, M. L.; Deacon, G. B.; Forsyth, C. M.; Junk, P. C.; Konstas, K.; Wang, J. *Chem.—Eur. J*. **2007**, *13*, 8092–8110.

(11) Bailey, B. C.; Huffman, J. C.; Mindiola, D. J. *J. Am. Chem. Soc*. **2007**, *129*, 5302–5303.

(12) Liu, W.; Welch, K.; Trindle, C. O.; Sabat, M.; Myers, W. H.; Harman, W. D. *Organometallics* **2007**, *26*, 2589–2597.

(13) Peterson, A. A.; McNeill, K. *Organometallics* **2006**, *25*, 4938–4940.

(14) Braun, T.; Schorlemer, V.; Neumann, B.; Stammler, H.-G. *J. Fluorine Chem*. **2006**, *127*, 367–372.

(15) Fuchibe, K.; Akiyama, T. *J. Am. Chem. Soc*. **2006**, *128*, 1434–1435.

 Published on Web 06/02/2010 © 2010 American Chemical Society

C−C bonds (CC coupling reactions),[6,8,15−17,19,20] C−O or C═O bonds,[10,14,25−28] C−Si bonds,[18] and C−B bonds (C−F bond borylation).[2,9]

C−F bond activation by osmium complexes is rare.[29−33] In the presence of fluoride as a catalyst, Me_3SiCF_3 exchanges CF_3 with the fluoride in the complex $[OsHF(CO)L_2]$ (L = P^iPr_3, P^tBu_2Me) to form the (difluorocarbene)(fluoro) complex $[OsHF(CF_2)(CO)L_2]$ via α-fluorine migration. This complex converts to $[OsF_2(CFH)(CO)L_2]$, resulting from exchange of one carbene fluoride with the hydride. Thus, the final osmium complex arises from a double α-fluorine migration.[31] Barrio and co-workers reported[30] that the hexahydride-osmium complex $[OsH_6(P^iPr_3)_2]$ reacts with fluorinated aromatic ketones in refluxing toluene to yield products involving the activation of *ortho* C−H and *ortho* C−F bonds on the aromatic ketones. For example, *ortho* C−F activation is preferred over *ortho* C−H activation for the reaction with 2,3,4,5,6-pentafluorobenzophenone to give the seven-coordinate complex $[\overline{OsH_3\{C_6F_4(CO)C_6H_5\}}(P^iPr_3)_2]$, and the corresponding reactions with pentafluoroacetophenone, decafluorobenzophenone, and 2,6-difluoroacetophenone to give $[OsH_3\{C_6F_4(CO)R\}(P^iPr_3)_2]$ (R = CH_3, C_6F_5) and $[\overline{OsH_3\{C_6H_3F(CO)CH_3\}}(P^iPr_3)_2]$, respectively. $[OsH_3Cl(P^iPr_3)_2]$ reacts with CH_2═CHF within the time of mixing to produce $[OsHFCl(\equiv CCH_3)(P^iPr_3)_2]$ and H_2.[29] Previously, we found[32,33] that the thermolysis reaction of the osmium(III) complex $[Os(SC_6F_5)_3(PMe_2Ph)_2]$ in refluxing toluene causes cleavage of *ortho* C−F bonds, affording $[Os(SC_6F_5)_2(S_2C_6F_4)(PMe_2Ph)]$ and $[Os(C_6F_5)_2(S_2C_6F_4)(PMe_2Ph)_2]$, but no Os−F complex was observed, and the fate of the exchanged fluorine atom remained unknown.

On the other hand, processes in transition metal−phosphane complexes that result in the unusual replacement of a phosphane substituent with F are relevant for C−F bond activation and have been recently reviewed by Macgregor.[34] Although rare, a number of well-defined examples of P−C/F exchange have been published, where a phosphane substituent is transferred from phosphorus to metal with the formation of the fluorophosphane complex. Experimental and computational mechanistic studies have examined the pathways involved in these reactions. These processes result in a net P−C/F exchange reaction, although this is sometimes masked by subsequent reactivity of the initial exchange product. For example, one of the first reports of this type describes the reaction of C_6F_6 with $[Ir(CH_3)(PEt_3)_3]$ that resulted in a process involving C−F bond cleavage, P−C bond cleavage, and P−F bond formation, yielding the complex *trans*-$[Ir(C_6F_5)(PFEt_2)(PEt_3)_2]$.[35] In this case not only the P−C/F exchange was involved but also the elimination of ethene and methane. Recent computational studies[36] of this reaction have shown that the phosphane ligands play an active role in this novel "phosphane-assisted" C−F activation process, involving nucleophilic attack of the electron-rich organometallic on the C_6F_6 and trapping of the displaced fluoride by a phosphane ligand to form a five-coordinated metallophosphorane intermediate. In other studies of C−F bond activation, the reaction of pentafluoropyridine with $[Pt(PR_3)_2]$ (R = cyclohexyl, isopropryl) in THF led to the unusual P−C/F exchange products $[PtR(4\text{-}C_5NF_4)(PFR_2)(PR_3)]$, while the corresponding reactions with $[Pd(PR_3)_2]$ yielded the classic C−F oxidative addition products $[PtF(4\text{-}C_5NF_4)(PR_3)_2]$.[37] Analogous P−C/F chemistry was observed for the reaction of C_6F_6 with $[Pt(PR_3)_2]$ and $[Pd(PR_3)_2]$.[38] Another P−C/F process was observed when $[RhF(PPh_3)_3]$ was heated in chlorobenzene to give the fluorophosphane complex *trans*-$[RhCl(PFPh_2)(PPh_3)_2]$ and biphenyl.[39] Mechanistic studies identified *cis*-$[RhPh(PFPh_2)(PPh_3)_2]$ as an intermediate, while kinetic studies showed that this species is formed via an intramolecular P−Ph/F exchange process.[38] DFT studies on the full $[RhF(PPh_3)_3]$ system[40] showed a clear preference for a pathway where the fluorine atom acts as an intramolecular nucleophile to give the five-coordinate metallophosphorane intermediate from which Ph migration to Rh completes the P−C/F exchange.

On the other hand, organo transition metal fluoro complexes have recently been studied due to their potential use in the synthesis of selectively fluorinated organic molecules. The progress in this area will depend on the investigation of the nature and reactivity of the transition metal−fluorine bond, which is far from being understood. For example, thermal treatment expected to result in reductive elimination from aryl metal fluoro complexes, stabilized by tertiary phosphanes, frequently led only to P−F bond forming

(16) Guo, H.; Kong, F.; Kanno, K.-I.; He, J.; Nakajima, K.; Takahashi, T. *Organometallics* **2006**, *25*, 2045–2048.
(17) Schaub, T.; Backes, M.; Radius, U. *J. Am. Chem. Soc.* **2006**, *128*, 15964–15965.
(18) Braun, T.; Izundu, J.; Steffen, A.; Neumann, B.; Stammler, H.-G. *Dalton Trans.* **2006**, 5118–5123.
(19) Korn, T. J.; Schade, M. A.; Wirth, S.; Knochel, P. *Org. Lett.* **2006**, *8*, 725–728.
(20) Steffen, A.; Sladek, M. I.; Braun, T.; Neumann, B.; Stammler, H.-G. *Organometallics* **2005**, *24*, 4057–4064.
(21) Jäger-Fiedler, U.; Arndt, P.; Baumann, W.; Spannenberg, A.; Burlakov, V. V.; Rosenthal, U. *Eur. J. Inorg. Chem.* **2005**, 2842–2849.
(22) Vela, J.; Smith, J. M.; Yu, Y.; Ketterer, N. A.; Flaschenriem, C. J.; Lachicotte, R. J.; Holland, P. L. *J. Am. Chem. Soc.* **2005**, *127*, 7857–7870.
(23) Aizenberg, M.; Milstein, D. *Science* **1994**, *265*, 359–361.
(24) Aizenberg, M.; Milstein, D. *J. Am. Chem. Soc.* **1995**, *117*, 8674–8675.
(25) Arroyo, M.; Bernès, S.; Cerón, M.; Cortina, V.; Mendoza, C.; Torrens, H. *Inorg. Chem.* **2007**, *46*, 4857–4867.
(26) Braun, T.; Rothfeld, S.; Schorlemer, V.; Stammler, A.; Stammler, H.-G. *Inorg. Chem. Commun.* **2003**, *6*, 752–755.
(27) Braun, T.; Steffen, A.; Schorlemer, V.; Neumann, B.; Stammler, H.-G. *Dalton Trans.* **2005**, 3331–3336.
(28) Braun, T.; Foxon, S. P.; Perutz, R. N.; Walton, P. H. *Angew. Chem., Int. Ed.* **1999**, *38*, 3326–3329.
(29) Ferrando-Miguel, G.; Gérard, H.; Eisenstein, O.; Caulton, K. G. *Inorg. Chem.* **2002**, *41*, 6440–6449.
(30) Barrio, P.; Castarlenas, R.; Esteruelas, M. A.; Lledós, A.; Maseras, F.; Oñate, E.; Tomàs, J. *Organometallics* **2001**, *20*, 442–452.
(31) Huang, D.; Koren, P. R.; Folting, K.; Davidson, E. R.; Caulton, K. G. *J. Am. Chem. Soc.* **2000**, *122*, 8916–8931.
(32) Arroyo, M.; Bernès, S.; Brianso, J. L.; Mayoral, E.; Richards, R. L.; Rius, J.; Torrens, H. *J. Organomet. Chem.* **2000**, *599*, 170–177.
(33) Arroyo, M.; Bernès, S.; Brianzo, J. L.; Mayoral, E.; Richards, R. L.; Rius, J.; Torrens, H. *Inorg. Chem. Commun.* **1998**, *1*, 273–276.
(34) Macgregor, S. A. *Chem. Soc. Rev.* **2007**, *36*, 67–76.
(35) Blum, O.; Frolow, F.; Milstein, D. *J. Chem. Soc., Chem. Commun.* **1991**, 258–259.
(36) Erhardt, S.; Macgregor, S. A. *J. Am. Chem. Soc.* **2008**, *130*, 15490–15498.
(37) Jasim, N. A.; Perutz, R. N.; Whitwood, A. C.; Braun, T.; Izundu, J.; Neumann, B.; Rothfeld, S.; Stammler, H.-G. *Organometallics* **2004**, *23*, 6140–6149.
(38) Macgregor, S. A.; Roe, D. C.; Marshall, W. J.; Bloch, K. M.; Bakhmutov, V. I.; Grushin, V. V. *J. Am. Chem. Soc.* **2005**, *127*, 15304–15321.
(39) Grushin, V. V.; Marshall, W. J. *J. Am. Chem. Soc.* **2004**, *126*, 3068–3069.
(40) Macgregor, S. A.; Wondimagegn, T. *Organometallics* **2007**, *26*, 1143–1149.

Scheme 1

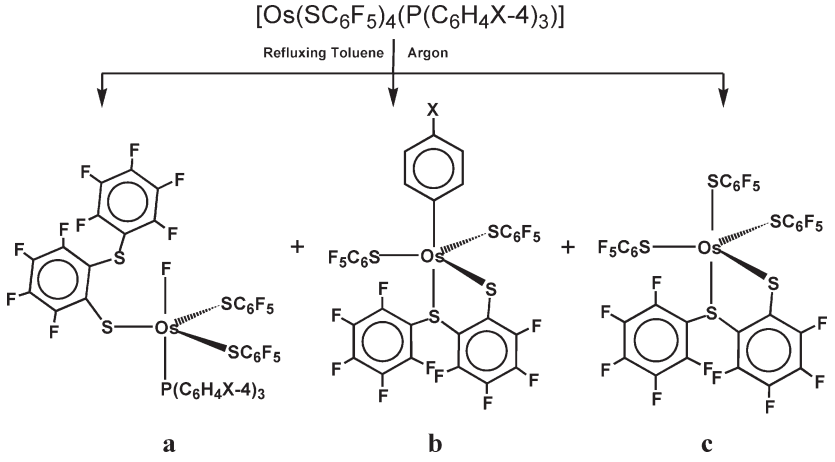

reactions, rather than the desired Ar−F reductive elimination. The fluorine-containing phosphorus products from reactions of these fluoro complexes have been identified as fluorophosphane coordinated to the metal or other uncoordinated fluorine-containing phosphorus products.[41]

A recent contribution to the development of aromatic C−F substitution reactions is the transition metal catalytic derivatization of C−F to C−S bonds.[7] In the presence of $[RhH(PPh_3)_4]$, 1,2-$(Ph_2P)_2C_6H_4$, and PPh_3, substituted fluorobenzenes, $X_nC_6H_{5-n}F$, react with disulfides (RSSR) to give the sulfides $X_nC_6H_{5-n}SR$. PPh_3 traps the fluorine to form PPh_3F_2. It was presumed that the fluoride transfer took place from the rhodium to the phosphorus atom of PPh_3. The authors suggested that the rhodium complex was involved in the cleavage of the C−F bond in the aryl fluorides and the S−S bond in the disulfides. The mode of C−F bond cleavage was a subject of interest, and nucleophilic aromatic substitution of the aryl fluoride with rhodium thiolate was proposed as a possible pathway. The authors emphasize that this rhodium-catalyzed method contains a notable mode of C−F activation by a transition metal catalyst and may offer an extremely broad scope for the manipulation of organosulfur compounds.

Here, we report a work centered on (phosphane)(fluorothiolate)osmium(IV) complexes, from which thermolysis reactions in refluxing toluene involves C−F bond activation with C−S bond formation to generate new complexes with a sulfide ligand and an Os−F bond as the first observed and isolated complexes. In addition, we have examined the products of subsequent rearrangements. Thus, heating in refluxing toluene causes the molecules of the starting compound to experience a series of complex rearrangements to give always well-defined products. The formation of all products involves the rupture of *ortho* C−F bonds from the original SC_6F_5 rings in the starting material, cleavage of P−C, C−S, Os−S, and Os−P bonds, and generation of new C−S, Os−C, and Os−F bonds. The results presented here contribute to our comprehension of the derivatization mechanism of fluorinated aryl groups via C−F activation and C−S bond formation at a transition metal center. Furthermore, fluoride complexes appear as key intermediates in catalytic cycles,[20] and therefore, investigations into the reactivity of these intermediates will improve our understanding and encourage further development of the functionalization of polyfluoroorganics.

Scheme 2

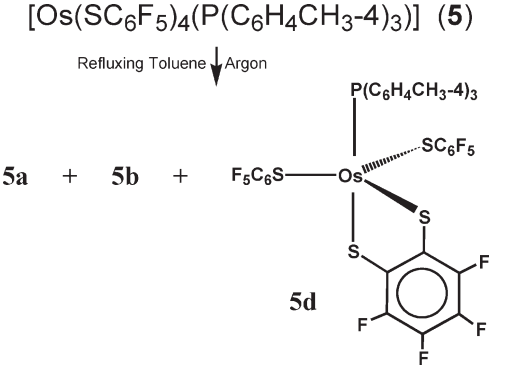

Results and Discussion

C−F bonds are broken during the thermolysis reactions of the osmium(IV) compounds $[Os(SC_6F_5)_4(P(C_6H_4\text{-}X\text{-}4)_3)]$ (X = CF_3 **1**, Cl **2**, F **3**, H **4**, CH_3 **5**, and OCH_3 **6**)[42] in refluxing toluene. The isolated products of these reactions are $[OsF(SC_6F_5)_2(SC_6F_4(SC_6F_5)\text{-}2)(P(C_6H_4X\text{-}4)_3)]$ (**1a**−**6a**), $[Os(SC_6F_5)_2(SC_6F_4(SC_6F_5)\text{-}2)(C_6H_4X\text{-}4)]$ (**2b**−**6b**), and the persulfured compound $[Os(SC_6F_5)_3(SC_6F_4(SC_6F_5)\text{-}2)]$ (**c**) previously reported[25] (Scheme 1), except for the reaction from **5**, which yields compounds **5a**, **5b**, and $[Os(SC_6F_5)_2(S_2C_6F_4)(P(C_6H_4CH_3\text{-}4)_3)]$ (**5d**) (Scheme 2).

TLC analysis showed that the first products observed after 1−2 h under reflux are compounds **a**. Compounds **b** and **c** are detected 1−3 h after compounds **a** appear. Yields of isolated compounds **a** varied between 20% and 50% after 6 h reaction

(41) (a) Grushin, V. V.; Marshall, W. J. *Organometallics* **2007**, *26*, 4997–5002. (b) Yandulov, D. V.; Tran, N. T. *J. Am. Chem. Soc.* **2007**, *129*, 1342–1358. (c) Marshall, W. J.; Grushin, V. V. *Organometallics* **2003**, *22*, 555–562. (d) Grushin, V. V.; Marshall, W. J. *Angew. Chem., Int. Ed.* **2002**, *41*, 4476–4479. (e) Geldbach, T. J.; Pregosin, P. S. *Eur. J. Inorg. Chem.* **2002**, 1907–1918. (f) J. den Reijer, C.; Dotta, P.; Pregosin, P. S.; Albinati, A. *Can. J. Chem.* **2001**, *79*, 693–704. (g) Grushin, V. V. *Organometallics* **2000**, *19*, 1888–1900. (h) J. den Reijer, C.; Wörle, M.; Pregosin, P. S. *Organometallics* **2000**, *19*, 309–316. (i) Morris, R. H.; Sawyer, J. F.; Schweitzer, C. T.; Sella, A. *Organometallics* **1989**, *8*, 2099–2106.

(42) Arroyo, M.; Mendoza, C.; Bernès, S.; Torrens, H.; Morales-Rojas, H. *Polyhedron* **2009**, *28*, 2625–2634.

Scheme 3

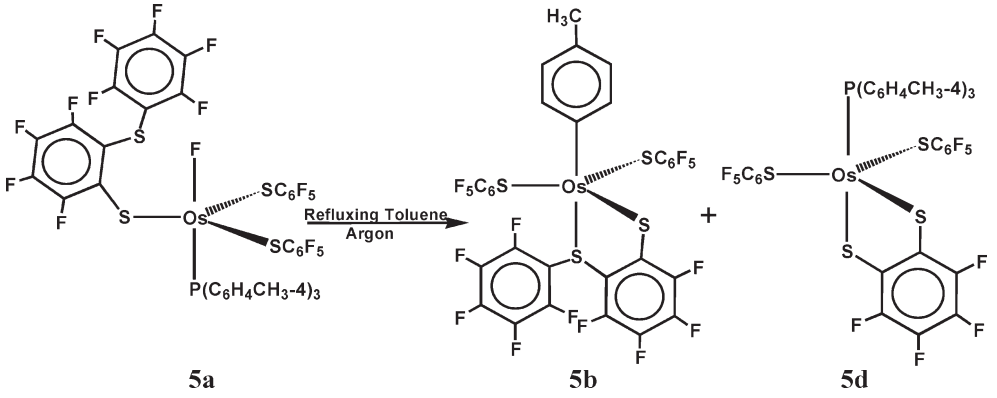

times. These yields are notably reduced when the reaction time is prolonged to increase the yields of compounds **b**. The yields of compounds **b** were 10−14% after 20 h reaction times. In the reaction from **5** (X = CH_3), where compound **c** is not detected, compound **5d** is observed instead, after 13 h of reaction time. Compounds **c** and **d** are produced in very low yields (2−4%).

Note that compounds **1a**−**6a** are isomers of their corresponding starting complexes **1**−**6**. Thermolysis reaction of the isolated compound $[OsF(SC_6F_5)_2(SC_6F_4(SC_6F_5)\text{-}2)(P(C_6H_4CH_3\text{-}4)_3)]$ (**5a**) in refluxing toluene gives rise to compounds $[Os(SC_6F_5)_2(SC_6F_4(SC_6F_5)\text{-}2)(C_6H_4CH_3\text{-}4)]$ (**5b**) and $[Os(SC_6F_5)_2(S_2C_6F_4)(P(C_6H_4CH_3\text{-}4)_3)]$ (**5d**) (Scheme 3). This result is consistent with the TLC results and suggests that compounds **a** are the initial products and that compounds **b**, as well as compounds **c** and **d**, likely arise from compounds **a**.

All these metallic reaction products were isolated by column chromatography.

In solution, compounds **a** are air-sensitive, and therefore their solutions were immediately evaporated under vacuum or stored under argon. The crystallization of **4a** and **5a** was carried out by a slow argon flux over hexane−CH_2Cl_2 (1:9) solutions. The isolation of compounds **b** was difficult due to the similar retention factors of compounds **b** and **c** (or **5d**) and unreacted starting material. However, reasonable isolations of compounds **b**−**d** were attained, as supported by the analytical data and NMR spectra. Compounds **b**, **c**, and **5d** were crystallized from air-stable hexane−CH_2Cl_2 (4:1) solutions.

The reaction from compound **5** (X = CH_3) yields **5d** instead of **c**, but there was no evidence to indicate the reason for this difference. The yield of compound **5d** is so low that it is probable that the level of possible compounds **1d**, **2d**, **3d**, **4d**, and **6d** was undetectable.

The products were characterized by elemental analysis, FAB^+ mass spectrometry, and NMR and IR spectroscopy. The FAB^+ mass spectra of all compounds $[OsF(SC_6F_5)_2(SC_6F_4(SC_6F_5)\text{-}2)(P(C_6H_4X\text{-}4)_3)]$ (**a**) show signals corresponding to $[M - F]^+$ ions with intensities of 18−95%. $[M - SC_6F_5]^+$ ions were present with intensities of 14−90%. Signals corresponding to $[M - (SC_6F_4(SC_6F_5))]^+$ (3 −19%), $[M - F - (SC_6F_5) - (P(C_6H_4X\text{-}4)_3)]^+$ (1−15%), $[M - F - (SC_6F_5) - (P(C_6H_4X\text{-}4)_3) - (C_6F_5)]^+$ (2−18%), and $[P(C_6H_4X\text{-}4)_3]^+$ (100%) were also detected.

The FAB^+ mass spectra of all compounds $[Os(SC_6F_5)_2(SC_6F_4(SC_6F_5)\text{-}2)(C_6H_4X\text{-}4)]$ (**b**) showed signals corresponding to the parent ions $[M]^+$ (1−17%) and signals corresponding to losses of different groups from the molecular ion including $[M - C_6H_4X]^+$ (3−42%), $[M - (SC_6F_5)]^+$ (3−44%), $[M - (SC_6F_5) - (C_6H_4X)]^+$ (8−80%), and $[M - (SC_6F_5) - (C_6H_4X) - (C_6F_5)]^+$ (2−26%).

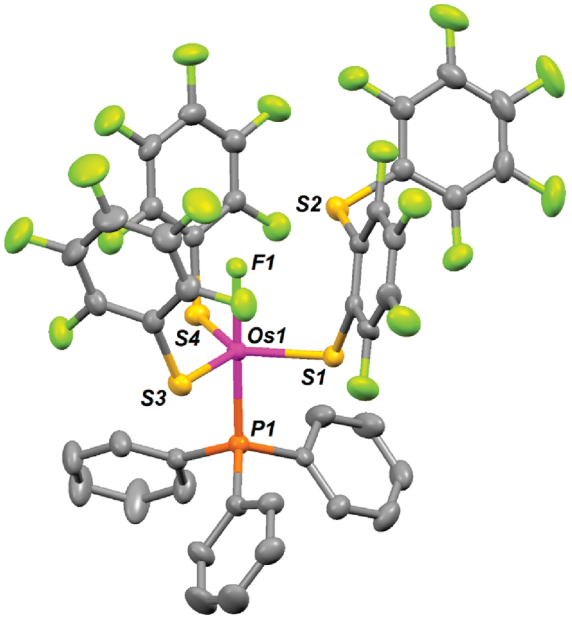

Figure 1. Molecular structure of compound **4a** with displacement ellipsoids at the 25% probability level. H atoms have been omitted for clarity. Main metric parameters (Å, deg): Os1−P1 2.3256(17), Os1−S1 2.2051(18), Os1−S3 2.1991(16), Os1−S4 2.2070(18), Os1−F1 2.041(3); P1−Os1−F1 178.79(10).

The FAB^+ mass spectra of compound $[Os(SC_6F_5)_3(SC_6F_4(SC_6F_5)\text{-}2)]$ (**c**) are as previously reported.[25]

The corresponding FAB^+ mass spectrum of compound $[Os(SC_6F_5)_2(S_2C_6F_4)(P(C_6H_4CH_3\text{-}4)_3)]$ (**5d**) showed the signal of the molecular ion $[M]^+$ (38%). The loss of SC_6F_5 is also observed (12%) as well as successive losses of C_6F_5 and H to generate $[M - (SC_6F_5) - (C_6F_5) - H)]^+$ (10%). Other fragments of lower intensities were also observed.

Single-crystal X-ray diffraction studies of compounds **4a**−**5a**, **2b**−**6b**, and **5d** indicated a common coordination geometry that resembles trigonal-bipyramidal geometry, with the equatorial plane containing three S atoms. Compounds **a**, **b**, and **d** have different axial components: P(phosphane) and F in compounds **a**, S and C(aryl) in compounds **b**, and S and P(phosphane) in compound **5d**.

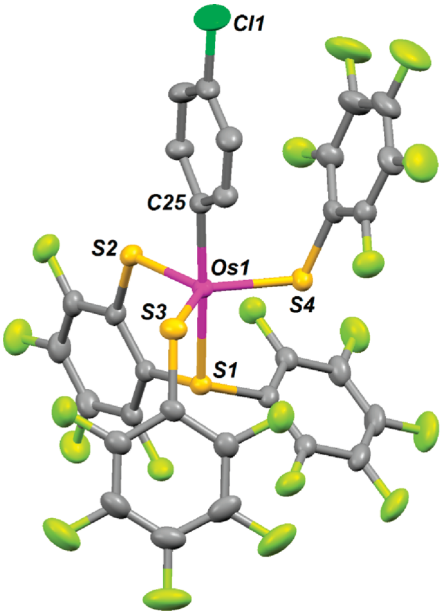

Figure 2. Molecular structure of compound **2b** with displacement ellipsoids at the 25% probability level. H atoms have been omitted for clarity. Main metric parameters (Å, deg): Os1−S1 2.4465(12), Os1−S2 2.1877(13), Os1−S3 2.2058(13), Os1−S4 2.2144(14), Os1−C25 2.109(5); S1−Os1−C25 177.06(15).

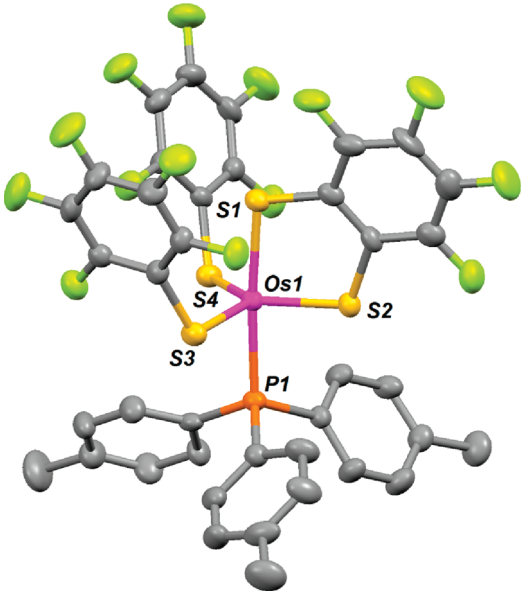

Figure 3. Molecular structure of compound **5d** with displacement ellipsoids at the 25% probability level. H atoms have been omitted for clarity. Main metric parameters (Å, deg): Os1−P1 2.386(2), Os1−S1 2.382(2), Os1−S2 2.190(2), Os1−S3 2.224(2), Os1−S4 2.225(2); P1−Os1−S1 175.73(8).

ORTEP-style views are shown for compounds **4a**, **2b**, and **5d** in Figures 1−3. However, regardless of the axial components, the *trans* angles remain close (175.17(9)−178.79(10)°) to the ideal value of 180°. All compounds also crystallize in a single space group, $P\bar{1}$, with similar cell parameters, indicating that the general shape of the molecules is not dependent on the exact nature of the ligands and that the molecules are packed at the solid-state van der Waals distances without significant intermolecular interactions.

The Os−F bond has been described previously[43−45] and has been X-ray measured in Os(IV) compounds, mainly in octahedral anions $[OsF_6]^{2-}$ and $[OsCl_2F_4]^{2-}$ and analogous hexahalide ions.[44,45] Bond lengths measured for compounds **4a** (2.041(3) Å) and **5a** (2.060(3) Å) are longer than those previously reported (ca. 1.92 Å).[44,45] This is to be expected due to the stronger *trans* influence of phosphane compared to halide ions. Thus, the fluoride ion in compounds **4a** and **5a** is likely weakly bonded to the metal center. The monocoordinated thiolate-thioether ligand in **4a** and **5a** is placed in the opposite hemisphere of the phosphane, in an arrangement resembling the starting complex.[46,42] In compounds $[OsF(SC_6F_5)_2(SC_6F_4(SC_6F_5)\text{-}2)(P(C_6H_4X\text{-}4)_3)]$ (**4a**, X = H; **5a**, X = CH_3), the Os−P bond length (2.3256(17) and 2.3348(15) Å, respectively) is shorter than the Os−P bond length in their respective starting compounds **4** (2.403(2) to 2.410(2) Å)[46] and **5** (2.4035(14) Å).[42] This shorter bond length reflects the weaker *trans* influence of the fluoride ligand relative to the thiolate ligand.

Except for **1b**, all **b** compounds have been characterized by X-ray analysis. The thiolate-thioether ligand, which was monocoordinated in compounds **a**, is now a chelating ligand, as it is in compound **c**, which we previously described.[25] In the *trans* position from the $S_{thioether}$ atom, an axial aryl group provided by the phosphane of the starting material is coordinated through a C atom, with Os−C bond lengths in the range 2.098(16)−2.112(3) Å. These Os−C bonds are longer than other Os(IV)−C bonds reported in the literature.[47] The trigonal-bipyramidal coordination geometry is completed by two thiolates, with their substituents arranged in an *anti* configuration relative to the equatorial plane. A configuration with both thiolate substituents oriented toward the hemisphere containing the thiolate-thioether ligand is unlikely, as the four perfluorinated rings would be sterically hindered. Conversely, an arrangement with both thiolate substituents placed in the other hemisphere seems to be at least as stable as the crystallized configuration.

In compounds $[\overline{Os(SC_6F_5)_2(SC_6F_4(SC_6F_5)\text{-}2)}(C_6H_4X\text{-}4)]$ (**2b**−**6b**), the distance Os−$S_{thioether(axial)}$ (2.445(4)−2.4532(10) Å) is longer than the distance Os−$S_{thioether(axial)}$ (2.3739(13) Å) in compound $[\overline{Os(SC_6F_5)_3(SC_6F_4(SC_6F_5)\text{-}2)}]$ (**c**),[25] reflecting the greater *trans* influence of the C_6H_4X-4 ligand relative to the SC_6F_5 ligand.

A remarkable characteristic of compounds **2b**−**6b** is their similarity in structure. Regardless of the identity of the phosphane present in the thermolyzed complex, the **b** compounds have identical ligand arrangements and almost identical molecular structures.

Finally, compound **5d** is analogous to a previously characterized Os(IV) compound bearing dimethylphenylphosphane[32,33] in place of tris-*p*-tolylphosphane. The 1,2-dithiolate-perfluorobenzene ligand acts as a chelate, with two S atoms occupying axial and equatorial positions, as the

(43) Ang, H. G.; Ang, S. G.; Leong, W. Y.; Winfield, J. *J. Fluorine Chem.* **1998**, *88*, 5–8.
(44) Kuppers, H.; Gobel, O.; Bruhn, C.; Schmahl, W. W. *Z. Kristallogr.* **2001**, *216*, 354–360.
(45) Bruhn, C.; Preetz, W. *Acta Crystallogr.* **1996**, *C52*, 321–325.
(46) Mendoza, C.; Bernès, S.; Arroyo, M. *Acta Crystallogr.* **2006**, *C62*, m201–m204.
(47) Eguillor, B.; Esteruelas, M. A.; Oliván, M.; Oñate, E. *Organometallics* **2004**, *23*, 6015–6024.

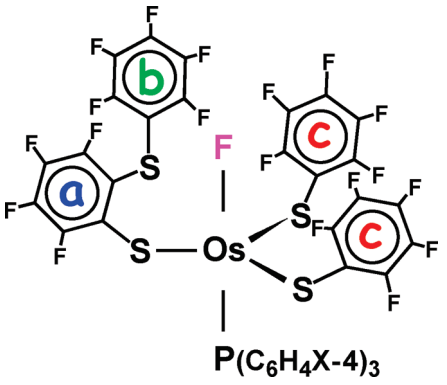

Figure 4. Drawing of $[OsF(SC_6F_5)_2(SC_6F_4(SC_6F_5)\text{-}2)(P(C_6H_4\text{-}X)_3)]$ (X = H, **4a**; X = CH_3, **5a**), as in the X-ray studies, showing the different phenyl rings.

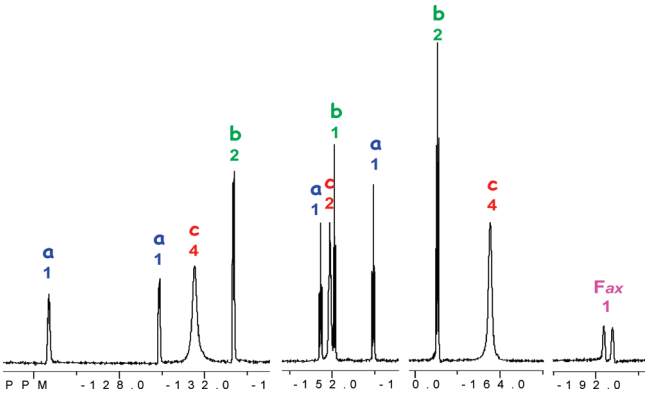

Figure 5. ^{19}F NMR spectrum of $[OsF(SC_6F_5)_2(SC_6F_4(SC_6F_5)\text{-}2)(P(C_6H_5)_3)]$ (**4a**) at 80 °C. The letter labels identify the signals that correspond to the same type of fluorinated ring, including the relative integrals.

thiolate-thioether ligand does in compounds **b** and **c**. Compound **5d** is related to the starting material $[Os(SC_6F_5)_4(P(C_6H_4Me\text{-}4)_3)]$, having the same coordination core, $[OsS_4P]$. The only difference is that four thiolates ($SC_6F_5^-$) are coordinated in the starting complex, while compound **5d**, which appears after the thermolysis has been carried out over a long time, has only three perfluorinated rings in the hemisphere occupied by the fluorinated ligands.

As expected, in compound $[Os(SC_6F_5)_2(S_2C_6F_4)(P(C_6H_4\text{-}CH_3\text{-}4)_3)]$ (**5d**), where the phosphane is *trans* to a sulfur of the dithiolate ligand, the Os−P bond length (2.386(2) Å) is longer than the corresponding Os−P bond length in compounds **4a** and **5a** (2.3256(17) and 2.3348(15) Å respectively), where the phosphane is *trans* to a fluoro ligand.

Furthermore, in compounds **2b**−**6b** and **5d**, the Os−$S_{equatorial}$ distances are notably shorter than the Os−S_{axial} distances, as expected for d^4-osmium(IV) complexes.[48]

NMR Studies of Compounds $[OsF(SC_6F_5)_2(SC_6F_4(SC_6F_5)\text{-}2)(P(C_6H_4X\text{-}4)_3)]$ (1a−6a). ^{19}F NMR Studies. At high temperatures, the ^{19}F NMR spectra are as expected assuming that the solid-state structure of compounds **a** (Figure 4) is retained in solution and that all the C_6F_5 rings are free to rotate about their C−S bonds. At 80 °C the ^{19}F NMR spectra recorded at 376 MHz (Figure 5) exhibit 10 absorptions in the perfluorinated aromatic region. One group of three resonances is due to the *ortho*, *para*, and *meta* fluorine atoms (relative intensities 4:2:4 at low, medium, and high fields, respectively)[49] from the two equivalent $^-SC_6F_5$ fragments (groups **c**, Figure 4). Another group of three resonances is due to the *ortho*, *para*, and *meta* fluorine atoms (relative intensities 2:1:2 at low, medium, and high fields, respectively) from the C_6F_5 ring of the ligand $^-SC_6F_4SC_6F_5$ (group **b**, Figure 4). A further group of four different resonances (relative intensities 1:1:1:1) is due to the fluorines in the C_6F_4 ring of the same $^-SC_6F_4SC_6F_5$ ligand (group **a**, Figure 4). In addition, all the spectra show a doublet at high field (relative intensity 1) corresponding to the *axial* fluoro ligand coupled to the *trans* phosphorus atom, $^2J_{F-P}$ in the range 148−158 Hz. At lower fields, the spectra of compounds **1a** (X = CF_3) and **3a** (X = F) exhibit additional resonances due to the fluorinated substituent on the phosphane ligand. A linear correlation is observed between the chemical shift of the *axial* fluorine and Tolman's electronic parameter[50] (χ) for the phosphane (Figure 6), consistent with the higher field chemical shift (more electronic protection) for the fluoro ligand *trans* to the more basic phosphane (lower Tolman's electronic parameter).

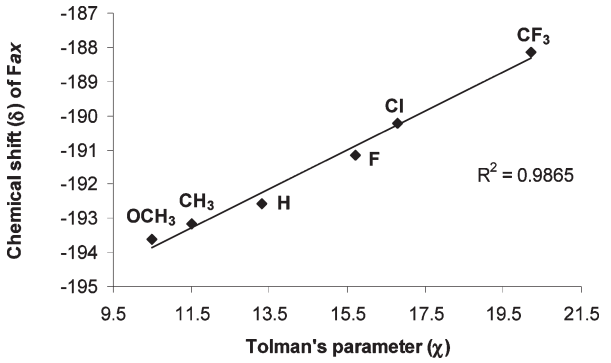

Figure 6. Plot of the F*ax*-chemical shift (δ) vs Tolman's parameter[50] for the phosphane (χ) in the compounds $[OsF(SC_6F_5)_2(SC_6F_4(SC_6F_5)\text{-}2)(P(C_6H_4X\text{-}4)_3)]$ (**1a**−**6a**).

$^{31}P\{^1H\}$ NMR Studies. As expected from the solid-state formulation of compounds **4a** and **5a** (Figure 4), the room-temperature $^{31}P\{^1H\}$ NMR spectra of compounds **1a**−**6a** exhibit a doublet signal due to magnetic coupling of the phosphorus with the *trans* fluoro ligand.

NMR Studies of Compounds $[OsF(SC_6F_5)_3(P(C_6H_4X\text{-}4)_3)]$ (1e, X = CF_3; 2e, X = Cl). ^{19}F NMR Studies. The ^{19}F NMR spectra of compounds **1a** (X = CF_3) and **2a** (X = Cl) exhibit additional resonances arising from minority compounds assigned to $[OsF(SC_6F_5)_3(P(C_6H_4CF_3\text{-}4)_3)]$ (**1e**) and $[OsF(SC_6F_5)_3(P(C_6H_4Cl\text{-}4)_3)]$ (**2e**). For both spectra, in the region of the *axial* fluorine, there is a second doublet (relative intensities between the major and minor doublets are 8:1 and 7:1, respectively). In the fluorinated aromatic region (Figure 7) there are three additional signals at low, medium, and high fields attributed to the *ortho*, *para*, and *meta* fluorine atoms (relative intensities ca. 6:3:6, respectively) of three equivalent equatorial $^-SC_6F_5$ ligands (see crystal structure of **2e**, Figure 8). In the CF_3 region of the spectrum of

(48) Rossi, A. R.; Hoffmann, R. *Inorg. Chem.* **1975**, *14*, 365–374.

(49) Bertrán, A.; García, J.; Martin, E.; Sosa, P.; Torrens, H. *Rev. Soc. Quím. Méx.* **1993**, *37* (4), 185–191. *Chem. Abstr.*, **1993**, *122*, 329084j.

(50) (a) Bartik, T.; Himmler, T.; Schulte, H.-G.; Seevogel, K. *J. Organomet. Chem.* **1984**, *272*, 29–41. (b) Tolman, C. A. *Chem. Rev.* **1977**, *77*, 313–348. (c) Tolman, C. A. *J. Am. Chem. Soc.* **1970**, *92*, 2953–2956.

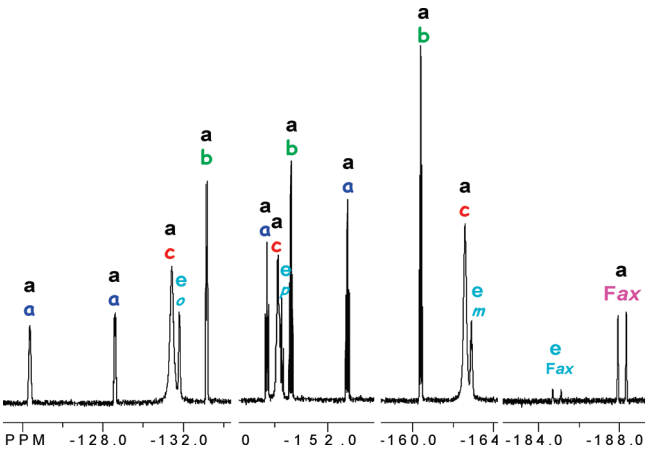

Figure 7. ^{19}F NMR spectrum of the mixture of $[OsF(SC_6F_5)_2(SC_6F_4(SC_6F_5)\text{-}2)(P(C_6H_4CF_3)_3)]$ (**1a**) and $[OsF(SC_6F_5)_3(P(C_6H_4CF_3)_3)]$ (**1e**) at 80 °C. The top letters identify the compound (**a** or **e**). The bottom letters identify the signals that correspond to each fluorinated ring in compound **1a** (same as in Figure 4) or that correspond to the *ortho*, *para*, and *meta* fluorine atoms in equivalent equatorial thiolates in compound **1e**. The two CF_3 signals at low field are omitted.

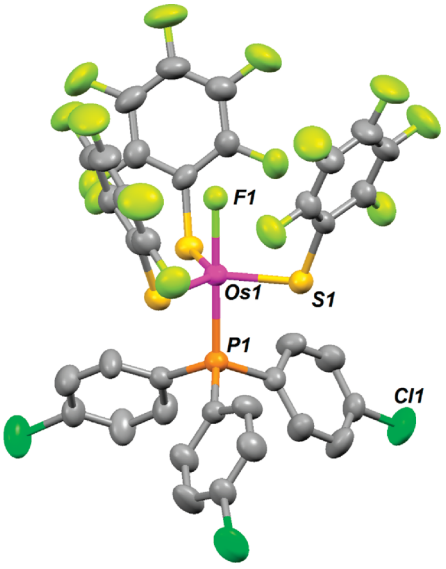

Figure 8. Molecular structure of compound **2e** with displacement ellipsoids at the 25% probability level. H atoms have been omitted for clarity. Main metric parameters (Å, deg): Os1−P1 2.332(3), Os1−S1 2.199(2), Os1−F1 2.055(6), P1−Os1−F1 180.

compound **1a**, there is also a singlet corresponding to **1e** (relative intensities between the major and minor CF_3 singlets 8:1).

The formation of compound **e** is consistent with the observation of compound **c** as products of a ligand redistribution reaction between two molecules **a**. It is worth noticing that the products **c** and **e** are both observed in similar low yields, as the redistribution reaction suggests.

To investigate more about compounds **1e** and **2e**, which have the same chromatographic retention factors as **1a** and **2a**, respectively, we have probed the recrystallization of the mixture "**2a** + **2e**" and, after repeated attempts, with decomposition of $[OsF(SC_6F_5)_2(SC_6F_4(SC_6F_5)\text{-}2)(P(C_6H_4Cl)_3)]$ (**2a**), we obtained a single crystal, of which the X-ray diffraction

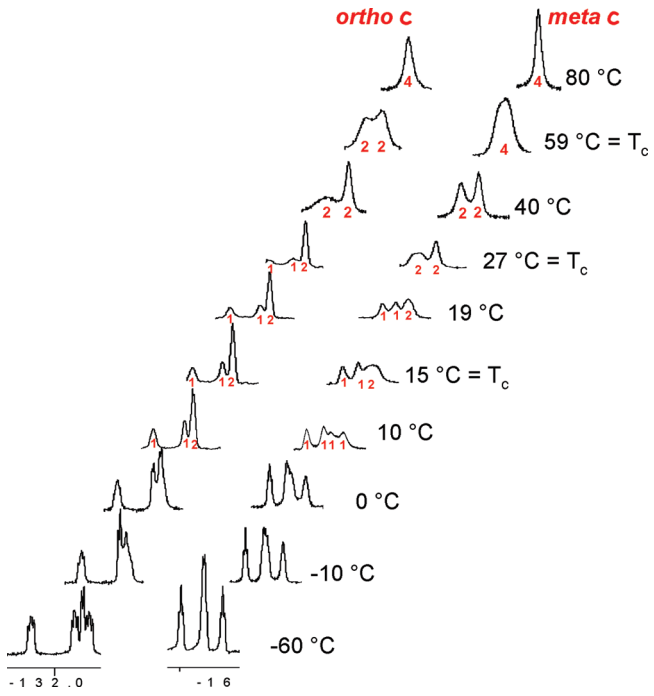

Figure 9. Variable-temperature ^{19}F NMR spectra of $[OsF(SC_6F_5)_2(SC_6F_4(SC_6F_5)\text{-}2)(P(C_6H_4CH_3\text{-}4)_3)]$ (**5a**) on the *ortho* and *meta* regions of the SC_6F_5 ligands (**c** groups), including relative integrals.

studies revealed the structure of the solvated complex $[OsF(SC_6F_5)_3(P(C_6H_4Cl)_3)]\cdot 1.38CH_2Cl_2$. The main molecule (Figure 8) displays a trigonal-bipyramidal coordination geometry for the Os center and a 3-fold symmetry, with the P−Os−F fragment lying on the crystallographic 3 axis. The C_6F_5 groups of all three equatorial thiolates are oriented in the direction of the F ligand (3-up orientation). The coordinated F^- ion, occupying an axial site, is thus located in a claw-shaped cavity with C_3 symmetry. The crystal contains large voids of ca. 250 Å^3, which were assumed to be filled with disordered CH_2Cl_2 molecules, used as a solvent in crystallization. The lattice solvent content was estimated through the SQUEEZE procedure. As the anion F^- is known as the ligand having the weakest *trans* influence, the axial phosphane in **2e** is strongly bonded to the metal center, as reflected in the rather short bond length Os1−P1 = 2.332(3) Å.

At room temperature, the COSY $^{19}F-^{19}F$ NMR spectra of **1a**−**6a** show couplings in the **b**-C_6F_5 ring and in the **a**-C_6F_4 ring. However, couplings corresponding to the signals of the **c**-C_6F_5 rings are absent due to fluxional processes of these groups. At −60 °C, the COSY $^{19}F-^{19}F$ NMR spectra show, in addition, the couplings corresponding to the signals of the **c**-C_6F_5 rings.

Spectra collected at room temperature are more complex than those collected at 80 °C. Variable-temperature ^{19}F NMR analysis of compound **5a** (X = CH_3) gives interesting results (Figures 9−11). As the temperature decreases, the subspectra of the **a** and **b** rings of the $^-SC_6F_4SC_6F_5$ ligand remain essentially unchanged, whereas the subspectra of the **c** rings of the two thiolate groups $^-SC_6F_5$ experience several modifications. Figure 9 shows that, as the temperature decreases, the *ortho* (4) and *meta* (4) signals from the two **c** rings collapse, each one giving rise to a pair of signals (relative intensities 2:2 and 2:2) at 62 and 59 °C, respectively.

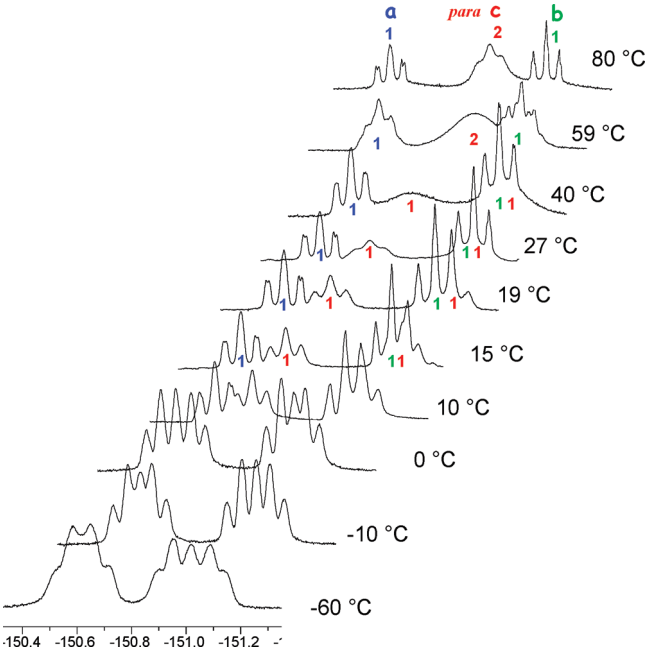

Figure 10. Variable-temperature ^{19}F NMR spectra of [OsF(SC$_6$F$_5$)$_2$(SC$_6$F$_4$(SC$_6$F$_5$)-2)(P(C$_6$H$_4$CH$_3$)$_3$)] (**5a**) on the *para* region of the SC$_6$F$_5$ ligands (**c** groups), including relative integrals.

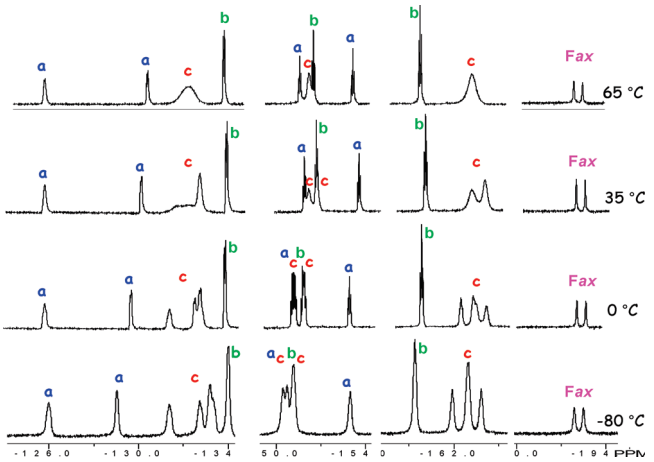

Figure 11. Full ^{19}F NMR spectra of [OsF(SC$_6$F$_5$)$_2$(SC$_6$F$_4$-(SC$_6$F$_5$)-2)(P(C$_6$H$_4$CH$_3$-4)$_3$)] (**5a**) at 65, 35, 0, and −80 °C.

At 37 and 27 °C, the low-field peaks of these *ortho* and *meta* groups, respectively, then collapse too, giving rise to new pairs of signals (relative intensities 1:1:2 and 1:1:2). At lower temperatures, the high-field peaks of these *ortho* and *meta* groups then collapse to give new pairs of resonances (relative intensities 1:1:1:1 and 1:1:1:1). Analysis of the **c** *para* zone is more complicated due to the proximity of one reasonance **a** on the low-field side and one resonance **b** on the high-field side (Figure 10). At high temperature (80 °C) the *para* **c** resonance is a broad triplet. As the temperature decreases, the broad triplet becomes a broad singlet at about 59 °C and then collapses into two broad singlets at a temperature somewhere between 59 and 40 °C. At 40 °C, the high-field broad *para* **c** singlet overlaps one resonance **b**. From 27 to 15 °C, the lowest field peak of the *para* **c** singlet becomes more defined. At 19 and 15 °C the high-field *para* **c** signal also appears more defined. When the temperature is less than 15 °C,

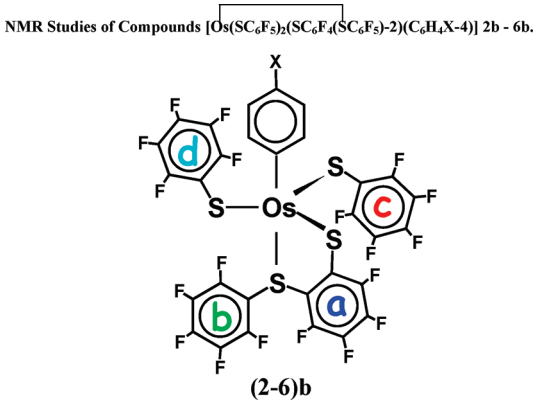

Figure 12. Drawing of [Os(SC$_6$F$_5$)$_2$(SC$_6$F$_4$(SC$_6$F$_5$)-2)(C$_6$H$_4$X-4)] (**2b**−**6b**), as in the solid state, showing the different phenyl rings. Although the NMR absorptions are linked to the aromatic rings **a**, **b**, **c**, and **d**, except for the rigid ring **a**, no definitive **b**, **c**, and **d** correspondence can be established.

the overlap of the two *para* **c** signals with the **a** signal (low field) and **b** signal (high field) prevents differentiation of the signals. The F*ax* resonance remains as only one doublet over the range of temperatures examined (Figure 11).

The effect of temperature on the NMR spectra can be explained with a molecule where, at high temperatures, rotation around the S1−C bond (Figure 1) renders the **c** rings chemically equivalent, and a free energy of activation for this process was estimated to be $\Delta G^{\ddagger} = 65 \pm 2$ kJ mol^{-1} from the variable-temperature NMR data. At lower temperatures, the rotation around the S4−C (or S3−C) bond of one **c** ring also becomes restricted, with an estimated $\Delta G^{\ddagger} = 58 \pm 2$ kJ mol^{-1}. With a further decrease in temperature, the rotation around the S3−C (or S4−C) bond of the another **c** ring also becomes restricted, with an estimated $\Delta G^{\ddagger} = 56 \pm 2$ kJ mol^{-1}.

NMR Studies of Compounds [Os(SC$_6$F$_5$)$_2$(SC$_6$F$_4$(SC$_6$F$_5$)-2)(C$_6$H$_4$X-4)] (2b−6b). ^{19}F NMR Studies. For compounds **2b**−**6b**, the COSY ^{19}F−^{19}F NMR spectra at different temperatures show four subspectra corresponding to three nonequivalent C$_6$F$_5$ groups (**b**, **c**, and **d** rings, Figure 12) and one C$_6$F$_4$ group (**a** ring, Figure 12). Figure 13 shows one of these COSY spectra at −20 °C.

Figure 14 shows the ^{19}F NMR spectra at −20 °C, RT, and +80 °C for compound **2b** (X = Cl). At −20 °C, the three subspectra of the groups C$_6$F$_5$ correspond to AA′BCC′ spin systems (relative intensities 1:1:1:1:1), while the subspectrum of the group C$_6$F$_4$ corresponds to an ABCD spin system (relative intensities 1:1:1:1). Thus, at −20 °C, all the spectra of compounds **b** exhibit 19 well-defined resonances of the same intensity, except for compound **3b** (X = F), which has an additional resonance at lower field arising from the fluorine atom of the C$_6$H$_4$F$^-$ ligand. At room temperature the number of signals is maintained; however two *ortho* and two *meta* signals are broad with low intensities, which are arbitrarily assigned to ring **c**. At 80 °C, the spectra show only one **c** *ortho* resonance (relative intensity 2, instead of two signals 1:1 at lower temperatures), one **c** *meta* resonance (relative intensity 2), one **d** *ortho* resonance (relative intensity 2), and one **d** *meta* resonance (relative intensity 2). These spectra at 80 °C are consistent with free rotation about C−S bonds in two C$_6$F$_5$ groups (**c** and **d**), but restricted rotation for the third C$_6$F$_5$ group (**b**) and the chelating C$_6$F$_4$ group (**a**).

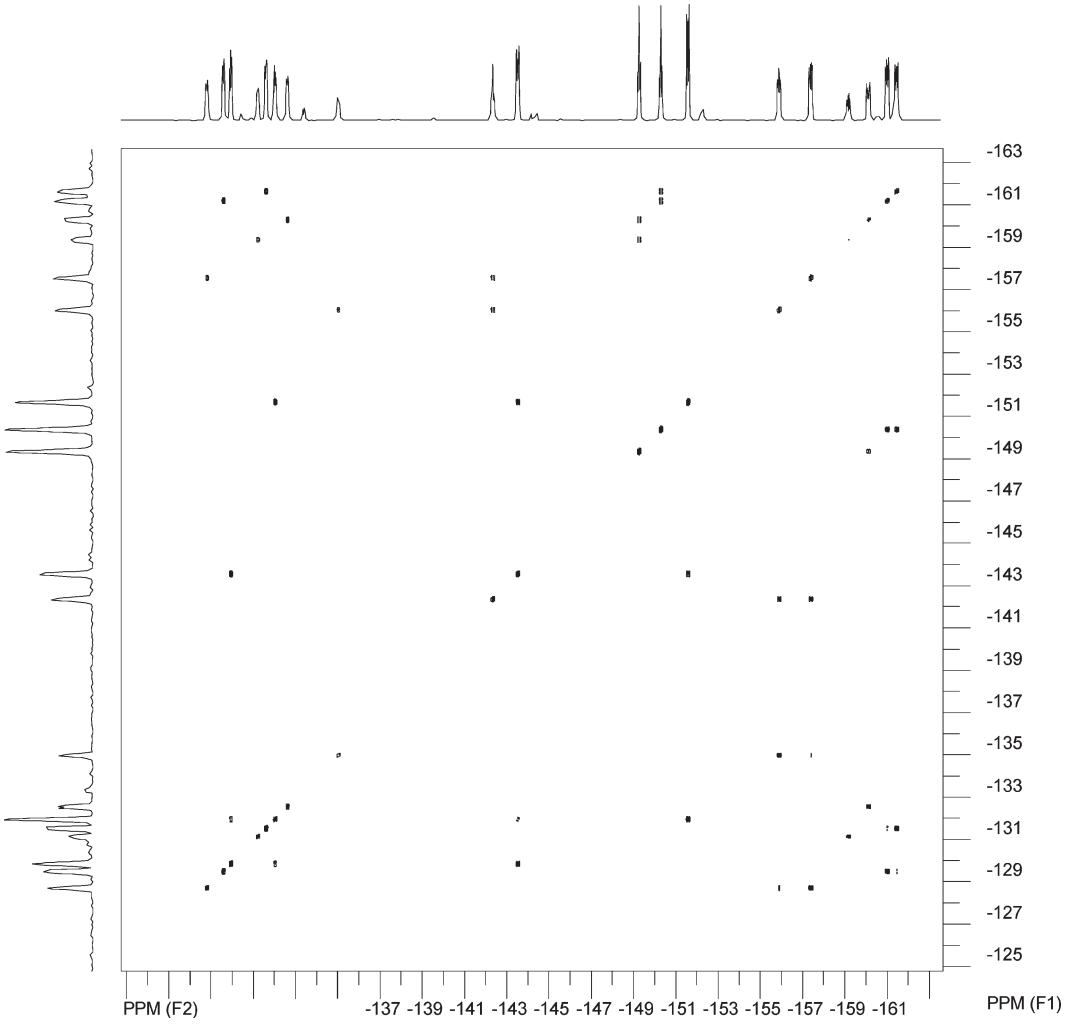

Figure 13. COSY $^{19}F-^{19}F$ NMR spectrum of $[Os(SC_6F_5)_2(SC_6F_4(SC_6F_5)\text{-}2)(C_6H_4Cl\text{-}4)]$ (**2b**) at −20 °C (minor signals correspond to **c** impurity).

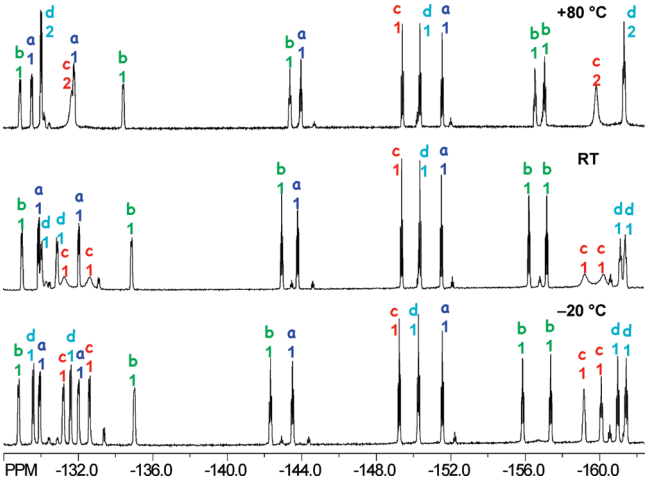

Figure 14. ^{19}F NMR spectra of $[Os(SC_6F_5)_2(SC_6F_4(SC_6F_5)\text{-}2)(C_6H_4Cl\text{-}4)]$ (**2b**) at 80 °C, RT, and −20 °C. The letter labels identify the signals that correspond to the same fluorinated ring, including the relative integrals (minor signals correspond to **c** impurity).

Indeed, rotation in the **b** C_6F_5 and **a** C_6F_4 groups is restricted within the full range of temperatures measured from −80 to +80 °C (relative intensities are 1:1:1:1:1 and 1:1:1:1 at all temperatures).

Analysis of the *meta* absorptions in the ^{19}F NMR spectra from −80 to +80 °C (Figure 15) was used to calculate the free energies of activation for the rotation around the C−S bond of both **c** and **d** C_6F_5 groups. The corresponding free energies of activation for the compounds **2b**−**6b** are in the range 58−59 ± 2 kJ mol^{-1} for groups **c** (S3-C or S4-C or S1-C7, Figure 2) and in the range 62−63 ± 2 kJ·mol^{-1} for groups **d** (S4-C or S3-C or S1-C7, Figure 2). Although the NMR absorptions are linked to the aromatic rings **a**, **b**, **c**, and **d**, except for the rigid ring **a**, no definitive **b**, **c**, and **d** correspondence can be established.

Summary Section

Previously, we found that the thermolysis reaction of $[Os(SC_6F_5)_3(PMe_2Ph)_2]$ in refluxing toluene causes an oxidative-rearrangement reaction affording $[Os(SC_6F_5)_2(S_2C_6F_4)(PMe_2Ph)]$ and $[Os(C_6F_5)_2(S_2C_6F_4)(PMe_2Ph)_2]$. This reaction involves phosphane dissociation, cleavage of an *ortho* C−F bond at a thiolate ligand, and transfer of a sulfur atom along with oxidation of the metal center.[32,33] However, neither Os−F nor Os−aryl/alkyl(from phosphane) complexes were yielded, and the fate of the exchanged fluorine

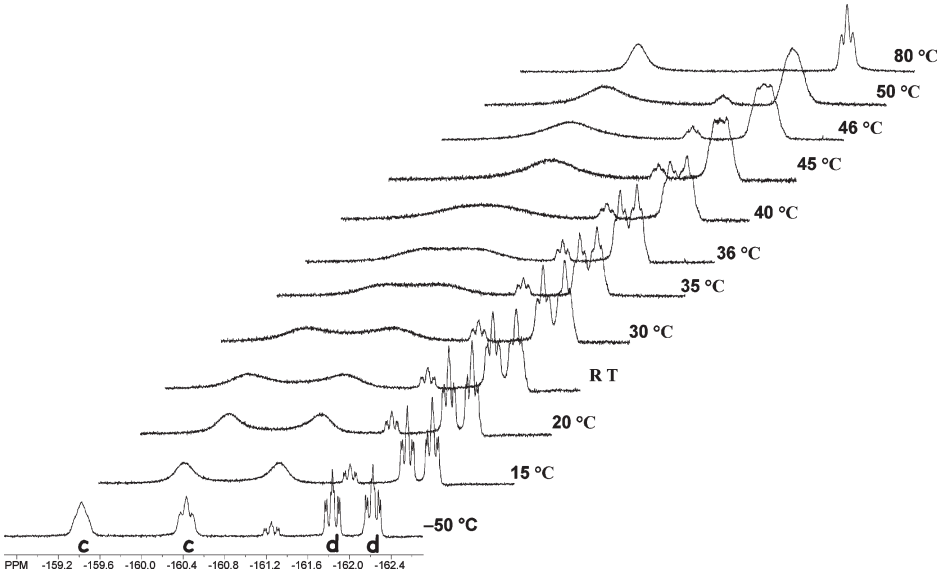

Figure 15. Variable-temperature ^{19}F NMR spectra of $[\overline{Os(SC_6F_5)_2(SC_6F_4(SC_6F_5)\text{-}2)}(C_6H_4OCH_3\text{-}4)]$ (**6b**) on the *meta* region of the **c** and **d** groups (minor signals correspond to **c** impurity).

atom remained unknown. The related thermolysis reactions of the compounds $[Os(SC_6F_5)_4(P(C_6H_4X\text{-}4)_3)]$ reported here show that the first products observed by TLC (compounds **a**) contain a fluorine atom directly bonded to the metal center. In fact, compounds **a** are isomers of the starting complexes, likely arising from an intramolecular rearrangement resulting in displacement of an *ortho* fluorine from a $^{-}SC_6F_5$ ligand by another $^{-}SC_6F_5$ group with formation of the new ligand $\{SC_6F_4(SC_6F_5)\text{-}2\}^{-}$. All compounds **a**, **b**, and **c** contain the $\{SC_6F_4(SC_6F_5)\text{-}2\}^{-}$ ligand. The thioether-sulfur of this ligand is coordinated to the osmium center in compounds **b** and **c**, but not in compounds **a**.

Compounds **b** may originate from compounds **a** by an exchange of P−C/F, with coordination of the $S_{thioether}$ and loss of coordination of the resulting fluorophosphane.

Compound **d**, obtained only through the thermolysis reaction of **5**, may originate from compound **a** by displacement of the fluorine ligand by coordination of the $S_{thioether}$.

A sequence of reactions for the formation of compounds **a**, **b**, and **d** is suggested in Scheme 4.

Compounds **c** and **e**, which are obtained in similar low yields, may originate through a ligand redistribution reaction between two molecules **a**, as suggested in Scheme 5.

The thermolysis reaction of the isolated $[OsF(SC_6F_5)_2(SC_6F_4(SC_6F_5)\text{-}2)(P(C_6H_4CH_3\text{-}4)_3)]$ (**5a**) to give $[\overline{Os(SC_6F_5)_2(SC_6F_4(SC_6F_5)\text{-}2)}(C_6H_4CH_3\text{-}4)]$ (**5b**) and $[Os(SC_6F_5)_2(S_2C_6F_4)(P(C_6H_4CH_3\text{-}4)_3)]$ (**5d**) also indicates that compounds **a** could be the initial thermolysis products, and compounds **b** (as well as compounds **c** and **d**) could then be formed from compounds **a**.

X-ray diffraction studies indicate that the monocoordinated thiolate-thioether ligand in compounds **4a** and **5a** is found in the hemisphere opposite the phosphane, in an arrangement resembling the starting complex.[46,42] This arrangement suggests that the first step of the C−F bond activation occurs in this hemisphere, without inversion at the equatorial S thiolate atoms. Although in compounds **4a** and **5a** the fluoride bound to the Os center survives TLC analysis and preparative column separation on silica gel, based on the X-ray studies and air-sensitivity in solution, this

Scheme 4

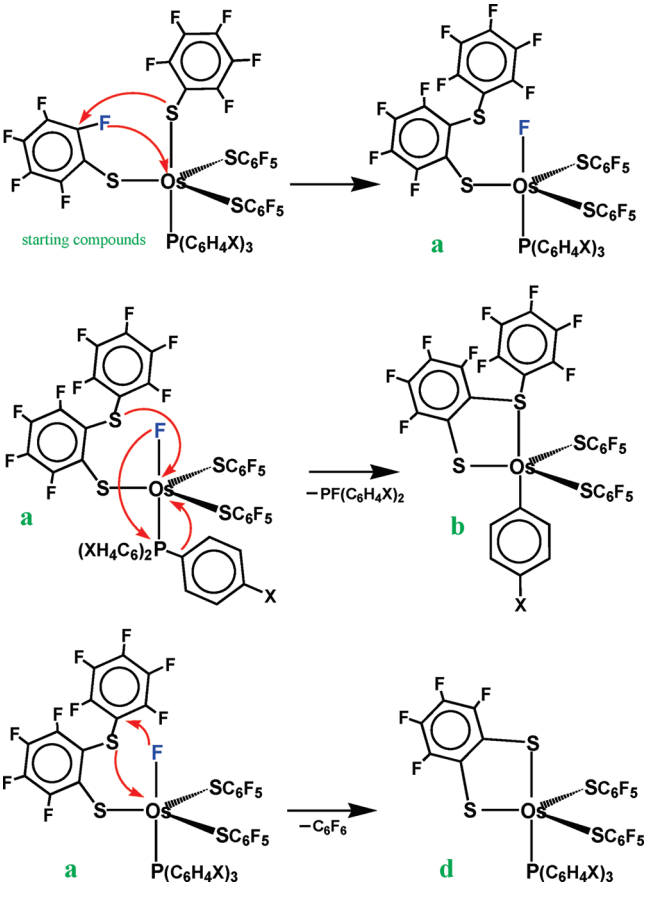

fluoro ligand probably is not tightly bonded enough to the metal center, which would facilitate an attack of the fluoro ligand at the phosphane to induce P−C bond cleavage during thermolysis (Scheme 4).

In a sealed NMR tube, $[Os(SC_6F_5)_4(P(C_6H_4Cl)_3)]$ (**2**) in $C_6D_5CD_3$ was heated with an oil bath at 110 °C. The solution was examined every two hours by $^{31}P\{^{1}H\}$ NMR at RT, but

Scheme 5

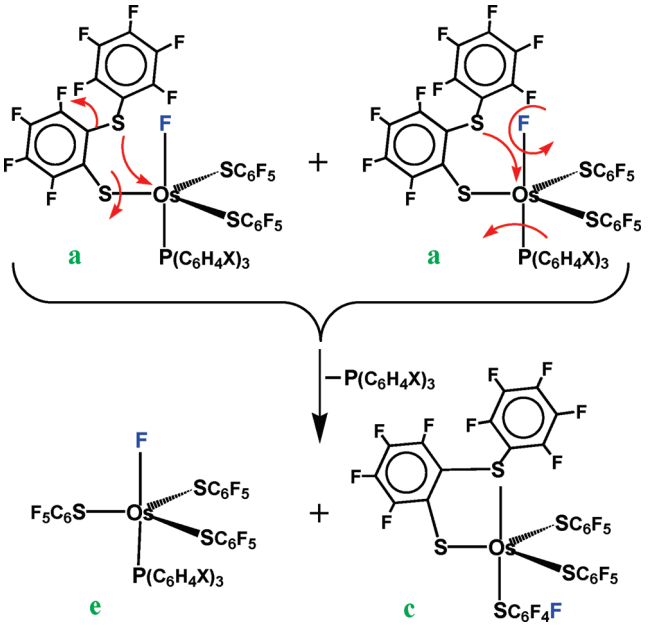

the spectra showed only the signals of the starting material[42] and a doublet corresponding to the formation of $[OsF(SC_6F_5)_2(SC_6F_4(SC_6F_5)\text{-}2)(P(C_6H_4Cl)_3)]$ (**2a**). There was no evidence of the presence of $PF(C_6H_4Cl)_2$ or $P(C_6H_4Cl)_3$ (possible byproducts in the formation of **2b**, **2e**, and **c**, Schemes 4 and 5). It is worth noting, however, that already in the normal reactions the yields of **2b**, **2e**, and **c** are low and that during the NMR experiment described above the cooling−heating cycles probably affect the normal outcome of this reaction. In addition, it has been documented that one analogue of the expected products, $PFPh_2$, disproportionates to Ph_2PF_3 and Ph_2PPPh_2. In turn Ph_2PF_3, with traces of water, gives rise to $Ph_2P(O)F$ and HF. The HF formed attacks the unreacted Ph_2PF to give Ph_2PF_2H.[51] This variety of probable phosphorus-containing byproducts in small proportions means that $^{31}P\{^1H\}$ NMR signals are weak to the point of being undetectable.

On the other hand, the C_6F_6 byproduct expected only in the thermolysis reaction of **5** was detected by GC-MS in the formation of the compound analogous to **5d**, $[Os(SC_6F_5)_2(S_2C_6F_4)(PMe_2Ph)]$.[32,33] In the present work, the yield of **5d** is again very low after a prolonged reaction time (see Experimental Section) and combined with the huge number of ^{19}F NMR signals in the reaction mixture (complexes **5**, **5a**, **5b**, and **5d**), and their partial overlap precludes its unequivocal identification.

Therefore, Schemes 4 and 5 show a likely sequence to rationalize the results of these reactions, based on the experimental evidence described above.

Conclusion

The apparently innocent thermal reactions of $[Os(SC_6F_5)_4(P(C_6H_4X\text{-}4)_3)]$ (X = CF_3 **1**, Cl **2**, F **3**, H **4**, CH_3 **5**, and OCH_3 **6**) are in fact the initial point of a very complex system yielding unusual compounds bearing Os−F bonds. The starting thiolate ligands $^-SC_6F_5$ are systematically transformed into $C_6F_5SC_6F_4S^-$ and, when X = CH_3, also into 1,2-$S_2C_6F_4^{2-}$.

In each reaction, the heating in refluxing toluene causes that the molecules of the starting compound to experience a series of complex rearrangements to give always well-defined products. Thus, formation of all products involves the rupture of *ortho* C−F bonds from the original SC_6F_5 rings in the starting material, cleavage of P−C, C−S, Os−S, and Os−P bonds, and generation of new C−S, Os−C, and Os−F bonds. This behavior is exhibited in all the compounds of the series studied.

As shown by variable-temperature NMR studies, the new molecules are fluxional and capable of adopting different conformations of close configurational energies. It is probable that this mobility contributes to the different intermediates required to render the output compounds found.

Experimental Section

Materials and Methods. All reactions were carried out under argon using conventional Schlenk-tube techniques. TLC (Merck 5 × 7.5 cm^2 Kiesegel 60 F_{254}) was used to monitor the progress of the reactions under study with hexane−CH_2Cl_2 (4:1) as eluent. Complexes $[Os(SC_6F_5)_4(P(C_6H_4X\text{-}4)_3)]$ were prepared as recently published.[42] The products were separated by passage through a silica gel chromatographic column with a hexane−dichloromethane solution as eluent.

Melting points were obtained on a Fisher-Johns melting point apparatus.

IR spectra were recorded over the 4000−400 cm^{-1} range on a Magna-Nicolet 750 FT-IR spectrometer using KBr pellets. Data are expressed in wavenumbers (cm^{-1}) with relative intensities (vs = very strong, s = strong, m = medium, w = weak).

Positive ion FAB mass spectra were recorded on a Jeol JMS-SX102A mass spectrometer operated at an accelerating voltage of 10 kV. Samples were desorbed from a 3-nitrobenzyl alcohol (NOBA) matrix using 3 keV xenon atoms. Mass measurements in FAB are performed at a resolution of 3000 using magnetic field scans and the matrix ions as the reference material.

Elemental analyses were determined by Galbraith Laboratories Inc.

^{19}F, COSY $^{19}F-^{19}F$, and $^{31}P\{^1H\}$ NMR spectra were recorded on a Varian Mercury VX400 spectrometer operating at 376, and 162 MHz respectively. Chemical shifts are relative to CCl_3F $\delta = 0$ (^{19}F) and H_3PO_4 $\delta = 0$ (^{31}P) using $C_6D_5CD_3$ as solvent.

All the free energies of activation, $\Delta G^{\ddagger}$, reported in this paper were calculated with the Eyring equation from variable-temperature ^{19}F NMR data, estimating the rate constant at the coalescence temperature on the basis of the chemical shift difference at lower temperatures.

Reactions. The general method is described only for the case of $[Os(SC_6F_5)_4(P(C_6H_4Cl\text{-}4)_3)]$ **(2)**: A 0.200 g (0.15 mmol) sample of **2** was dissolved in toluene (20 mL). The stirred brown solution was refluxed for 6 h. After this time, the solvent was removed under vacuum, and the residue was purified by column chromatography (silica gel, hexane−CH_2Cl_2, 1:2). Two fractions were separated. The first fraction contains yet some of the starting compound **2** and only very low quantities of **2b** and **c**. From the second fraction, by evaporation of the eluent under vacuum at room temperature, is isolated a green powder that contains a mixture of **2a** and **2e** (0.080 g), both compounds with the same TLC retention factors. IR (KBr, cm^{-1}): 1513(vs), 1494(vs), 1446(s), 1397(s), 1088(vs), 979(s), 821(w), 750(w). FAB^+-MS {*m*/*z* (%) [fragment]}: 1333 (95) [M^+_{2a} − F], 1153 (90) [M^+_{2a} − (SC_6F_5)], 973 (27) [M^+_{2a} − ($SC_6F_4(SC_6F_5)$)], 770 (15)

(51) (a) Riesel, L.; Haenel, J. *Z. Anorg. Allg. Chem.* **1991**, *603*, 145–150. (b) Riesel, L.; Haenel, J. *J. Fluorine Chem.* **1988**, *38*, 335–340. (c) Brown, C.; Murray, M.; Schmutzler, R. *J. Chem. Soc. C* **1970**, 878–881. (d) Muetterties, E. L.; Mahler, W.; Schmutzler, R. *Inorg. Chem.* **1963**, *2*, 613–618. (e) Schmutzler, R. *J. Chem. Soc.* **1964**, 4551–4557.

$[M^+_{\mathbf{2a}} - F - (SC_6F_5) - (P(C_6H_4Cl)_3)]$, 603 (15) $[M^+_{\mathbf{2a}} - F - (SC_6F_5) - (P(C_6H_4Cl)_3) - (C_6F_5)]$, 364 (100) $[P(C_6H_4Cl)_3]^+$. $^{31}P\{^1H\}$ NMR ($C_6D_5CD_3$, RT), δ (ppm): δ −4.80 (d, $P(C_6H_4Cl\text{-}4)_3$). ^{19}F NMR spectra at 80 °C show the presence of **2a** and **2e**, in a ratio of 7:1.

[OsF(SC_6F_5)$_2$(SC_6F_4(SC_6F_5)-2)($P(C_6H_4Cl\text{-}4)_3$)] (2a). ^{19}F NMR ($C_6D_5CD_3$, 80 °C), δ (ppm): ring **a**, δ −124.66 (m, 7F, 7($1C_6F_4$)), −129.18 (m, 7F, 7($1C_6F_4$)), −150.50 (m, 7F, 7($1C_6F_4$)), −153.32 (m, 7F, 7($1C_6F_4$)); ring **b**, δ −133.29 (d, 14F*o*, 7($1C_6F_5$), $^3J_{Fo\text{-}Fm}$ = 23.3 Hz), −151.25 (t, 7F*p*, 7($1C_6F_5$), $^3J_{Fp\text{-}Fm}$ = 20.7 Hz), −160.64 (m, 14F*m*, 7($1C_6F_5$)); rings **c**, δ −131.56 (br s, 28F*o*, 7($2SC_6F_5$)), −150.88 (br t, 14F*p*, 7($2SC_6F_5$), $^3J_{Fp\text{-}Fm}$ = 17.7 Hz), −163.02 (br s, 28F*m*, 7($2SC_6F_5$)); F ligand, δ −190.21 (d, 7(1F*ax*), $^2J_{F\text{-}P}$ = 158 Hz).

[OsF(SC_6F_5)$_3$($P(C_6H_4Cl\text{-}4)_3$)] (2e). ^{19}F NMR ($C_6D_5CD_3$, 80 °C), δ (ppm): −131.95 (br s, 6F*o*, 3SC_6F_5), −151.05 (t, 3F*p*, 3SC_6F_5, $^3J_{Fp\text{-}Fm}$ = 20.7 Hz), −163.35 (m, 6F*m*, 3SC_6F_5); F ligand, δ −187.43 (d, 1F*ax*, $^2J_{F\text{-}P}$ = 157 Hz).

To increase the yield of **2b**, it was necessary to extend the time of the reaction to 22 h, decreasing to traces the yield of **2a** as a consequence. The solvent was removed under vacuum, and the residue was purified by column chromatography (silica gel, hexane−CH_2Cl_2, 4:1). The first fraction contains the compound **2b** and a second fraction contains the compounds **c** plus the unreacted starting **2**, additional passage through a new chromatographic column being required to separate compounds **c** and **2**.

[Os(SC_6F_5)$_2$(SC_6F_4(SC_6F_5)-2)(C_6H_4Cl-4)] (2b), was isolated from the corresponding fraction as brown needle crystals (0.022 g, 14%) by slow evaporation of the eluent at room temperature. Anal. Calcd for $C_{30}H_4ClF_{19}OsS_4$: C, 33.39; H, 0.37; S, 11.88. Found: C, 33.44; H, < 0.5; S, 12.06. Mp: 203 °C, dec. IR (KBr, cm^{-1}): 1515(vs), 1504(vs), 1485(vs), 1461(s), 1394(w), 1087(s), 979(s), 810(w). FAB$^+$-MS {*m*/*z* (%) [fragment]}: 1080 (3) M^+, 969 (10) $[M^+ - (C_6H_4Cl)]$, 881 (6) $[M^+ - (SC_6F_5)]$, 770 (41) $[M^+ - (SC_6F_5) - (C_6H_4Cl)]$, 603 (10) $[M^+ - (SC_6F_5) - (C_6H_4Cl) - (C_6F_5)]$, 436 (4) $[M^+ - (SC_6F_5) - (C_6H_4Cl) - 2(C_6F_5)]$. ^{19}F NMR ($C_6D_5CD_3$, RT), δ (ppm): ring **a**, δ −130.94 (ddd, 1F, C_6F_4, $^3J_{F\text{-}F}$ = 22.6 Hz, $^4J_{F\text{-}F}$ = 10.9 Hz, $^5J_{F\text{-}F}$ = 4.1), −133.13 (m, 1F, C_6F_4), −145.05 (td, 1F, C_6F_4, $^3J_{F\text{-}F}$ = 21.4 Hz, $^4J_{F\text{-}F}$ = 6.8 Hz), −152.9 (m, 1F, C_6F_4); ring **b**, δ −130.04 (m, 1F*o*, C_6F_5), −136.00 (d, 1F*o*′, C_6F_5, $^3J_{Fo\text{-}Fm}$ = 19.2 Hz), −144.19 (tt, 1F*p*, C_6F_5, $^3J_{Fp\text{-}Fm}$ = 22.2, $^4J_{Fp\text{-}Fo}$ = 5.6 Hz), −157.65 (td, 1F*m*′, C_6F_5, $^3J_{Fm\text{-}Fo/p}$ = 21.8 Hz), −158.60 (td, 1F*m*, C_6F_5, $^3J_{Fm\text{-}Fo/p}$ = 22.2 Hz, $^4J_{Fm\text{-}Fm}$ = 6.8 Hz); ring **c**, δ −132.35 (br s, 1F*o*, 1SC_6F_5), −133.71 (br s, 1F*o*′, 1SC_6F_5), −150.71 (t, 1F*p*, 1SC_6F_5, $^3J_{Fp\text{-}Fm}$ = 20.3 Hz), −160.71 (br s, 1F*m*, 1SC_6F_5), −161.69 (br s, 1F*m*′, 1SC_6F_5); ring **d**, δ −131.10 (d, 1F*o*, 1SC_6F_5, $^3J_{Fo\text{-}Fm}$ = 23.3 Hz), −131.94 (d, 1F*o*′, 1SC_6F_5, $^3J_{Fo\text{-}Fm}$ = 20.7 Hz), −151.71 (t, 1F*p*, 1SC_6F_5, $^3J_{Fp\text{-}Fm}$ = 20.7 Hz), −162.62 (t, 1F*m*, 1SC_6F_5, $^3J_{Fm\text{-}Fo/p}$ = 20.7 Hz), −162.9 (t, 1F*m*′, 1SC_6F_5, $^3J_{Fo\text{-}Fm}$ = 19.2 Hz).

Compound **c** was isolated in a very low yield, due to poor separation with respect to the starting complex **2** in the chromatographic column, and was identified as the green complex previously reported as [Os(SC_6F_5)$_3$(SC_6F_4(SC_6F_5)-2)][25] by FAB mass spectrometry.

Analogous reactions from **1** and **3**−**6** (0.200 g) afforded the next compounds (yields are from the corresponding isolated complexes):

Mixture of 1a and 1e: green powder (0.100 g), both compounds with the same TLC retention factors. IR (KBr, cm^{-1}): 1515(vs), 1497(vs), 1399(m), 1323(s), 1176(s), 1137(s), 1091(vs), 982(s), 706(w). FAB$^+$-MS {*m*/*z* (%) [fragment]}: 1435 (57) $[M^+_{\mathbf{1a}} - F]$, 1255 (59) $[M^+_{\mathbf{1a}} - (SC_6F_5)]$, 1075 (19) $[M^+_{\mathbf{1a}} - (SC_6F_4(SC_6F_5))]$, 770 (15) $[M^+_{\mathbf{1a}} - F - (SC_6F_5) - (P(C_6H_4CF_3)_3)]$, 603 (18) $[M^+_{\mathbf{1a}} - F - (SC_6F_5) - (P(C_6H_4CF_3)_3) - (C_6F_5)]$, 571 (15) $[M^+_{\mathbf{1a}} - F - 2(SC_6F_5) - (P(C_6H_4CF_3)_3)]$, 466 (100) $[P(C_6H_4CF_3)_3]^+$. $^{31}P\{^1H\}$ NMR ($C_6D_5CD_3$, RT), δ (ppm): −1.33 (d, $P(C_6H_4CF_3\text{-}4)_3$). ^{19}F NMR spectra at 80 °C show the presence of **1a** and **1e**, in a ratio of 8:1.

[OsF(SC_6F_5)$_2$(SC_6F_4(SC_6F_5)-2)($P(C_6H_4CF_3\text{-}4)_3$)] (1a). ^{19}F NMR ($C_6D_5CD_3$, 80 °C), δ (ppm): −64.13 (s, 72F, 8($1P(C_6H_4CF_3\text{-}4)_3$)); ring **a**, δ −124.38 (m, 8F, 8($1C_6F_4$)), −128.60 (m, 8F, 8($1C_6F_4$)), −149.72 (m, 8F, 8($1C_6F_4$)), −152.74 (m, 8F, 8($1C_6F_4$)); ring **b**, δ −133.15 (d, 16F*o*, 8($1C_6F_5$), $^3J_{Fo\text{-}Fm}$ = 24.8 Hz), −150.62 (t, 8F*p*, 8($1C_6F_5$), $^3J_{Fp\text{-}Fm}$ = 20.5 Hz), −160.40 (m, 16F*m*, 8($1C_6F_5$)); rings **c**, δ −131.41 (br s, 32F*o*, 8($2SC_6F_5$)), −150.14 (br t, 16F*p*, 8($2SC_6F_5$), $^3J_{Fp\text{-}Fm}$ = 20.3 Hz), −162.59 (br s, 32F*m*, 8($2SC_6F_5$)); F ligand, δ −188.14 (d, 8(1F*ax*), $^2J_{F\text{-}P}$ = 156 Hz).

[OsF(SC_6F_5)$_3$($P(C_6H_4CF_3\text{-}4)_3$)] (1e). ^{19}F NMR ($C_6D_5CD_3$, 80 °C), δ (ppm): δ −64.08 (s, 9F, $P(C_6H_4CF_3\text{-}4)_3$), δ −131.82 (br s, 6F*o*, 3SC_6F_5), −150.28 (t, 3F*p*, 3SC_6F_5, $^3J_{Fp\text{-}Fm}$ = 19.6 Hz), −162.91 (m, 6F*m*, 3SC_6F_5); F ligand, δ −184.90 (d, 1F*ax*, $^2J_{F\text{-}P}$ = 156 Hz).

A brown product labeled as **1b** (TLC analogous to the other compounds of type **b**) was observed both by TLC and in the chromatographic column, but it was not characterized because of its very low yield. Traces of compound **c** were also observed in this reaction and identified as [Os(SC_6F_5)$_3$(SC_6F_4(SC_6F_5)-2)][25] by TLC comparison with an authentic sample.

[OsF(SC_6F_5)$_2$(SC_6F_4(SC_6F_5)-2)($P(C_6H_4F\text{-}4)_3$)] (3a): green (0.044 g, 22%). Anal. Calcd for $C_{42}H_{12}F_{23}OsPS_4$: C, 38.72; H, 0.93; S, 9.84. Found: C, 38.53; H, 1.03; S, 9.86. Mp: 180 °C, dec. IR (KBr, cm^{-1}): 1514(vs), 1498(vs), 1447(s), 1398(w), 1243(s), 1089(vs), 980(s), 711(w). FAB$^+$-MS {*m*/*z* (%) [fragment]}: 1284 (35) $[M^+ - H - F]$, 1104 (24) $[M^+ - H - (SC_6F_5)]$, 925 (9) $[M^+ - (SC_6F_4(SC_6F_5))]$, 770 (3) $[M^+ - F - (SC_6F_5) - (P(C_6H_4F)_3)]$, 603 (4) $[M^+ - F - (SC_6F_5) - (P(C_6H_4F)_3) - (C_6F_5)]$, 316 (100) $[P(C_6H_4F)_3]^+$. ^{19}F NMR ($C_6D_5CD_3$, 80 °C), δ (ppm): −106.67 (s, 3F, $P(C_6H_4F\text{-}4)_3$); ring **a**, δ −124.78 (m, 1F, C_6F_4), −129.29 (m, 1F, C_6F_4), −150.64 (m, 1F, C_6F_4), −153.45 (m, 1F, C_6F_4); ring **b**, δ −133.35 (d, 2F*o*, C_6F_5, $^3J_{Fo\text{-}Fm}$ = 21.8 Hz), −151.33 (t, 1F*p*, C_6F_5, $^3J_{Fp\text{-}Fm}$ = 20.8 Hz), −160.73 (m, 2F*m*, C_6F_5); rings **c**, δ −131.63 (br s, 4F*o*, 2SC_6F_5), −151.01 (br t, 2F*p*, 2SC_6F_5), −163.08 (br s, 4F*m*, 2SC_6F_5); F ligand, δ −191.16 (d, 1F*ax*, $^2J_{F\text{-}P}$ = 156 Hz). $^{31}P\{^1H\}$ NMR ($C_6D_5CD_3$, RT), δ (ppm): −1.36 (d, 1P, $P(C_6H_4F\text{-}4)_3$).

[Os(SC_6F_5)$_2$(SC_6F_4(SC_6F_5)-2)(C_6H_4F-4)] (3b): brown plate crystals (0.018 g, 11%). Anal. Calcd for $C_{30}H_4F_{20}OsS_4$: C, 33.90; H, 0.36; S, 12.07. Found: C, 33.93; H, 0.58; S, 12.50. Mp: 215 °C, dec. IR (KBr, cm^{-1}): 1515(vs), 1506(vs), 1486(vs), 1462(s), 1394(w), 1232(s), 1087(s), 979(s). FAB$^+$-MS {*m*/*z* (%) [fragment]}: 1064 (1) M^+, 865 (5) $[M^+ - (SC_6F_5)]$, 770 (22) $[M^+ - (SC_6F_5) - (C_6H_4F)]$, 666 (5) $[M^+ - 2(SC_6F_5)]$, 603 (8) $[M^+ - (SC_6F_5) - (C_6H_4F) - (C_6F_5)]$, 571 (3) $[M^+ - 2(SC_6F_5) - (C_6H_4F)]$, 436 (3) $[M^+ - (SC_6F_5) - (C_6H_4F) - 2(C_6F_5)]$, 404 (1) $[M^+ - 2(SC_6F_5) - (C_6H_4F) - (C_6F_5)]$. ^{19}F NMR ($C_6D_5CD_3$, RT), δ (ppm): ring **a**, δ −129.88 (ddd, 1F, C_6F_4, $^3J_{F\text{-}F}$ = 22.7 Hz, $^4J_{F\text{-}F}$ = 11.7 Hz, $^5J_{F\text{-}F}$ = 4.1 Hz), −132.01 (m, 1F, C_6F_4), −143.84 (td, 1F, C_6F_4, $^3J_{F\text{-}F}$ = 22.0 Hz, $^4J_{F\text{-}F}$ = 6.8 Hz), −151.63 (m, 1F, C_6F_4); ring **b**, δ −128.94 (m, 1F*o*, C_6F_5), −134.84 (d, 1F*o*′, C_6F_5, $^3J_{Fo\text{-}Fm}$ = 19.2), −143.02 (t, 1F*p*, C_6F_5, $^3J_{Fp\text{-}Fm}$ = 21.8 Hz), −156.30 (td, 1F*m*′, C_6F_5, $^3J_{Fm\text{-}Fo/p}$ = 22.0 Hz, $^4J_{Fm\text{-}Fm}$ = 6.8 Hz), −157.26 (td, 1F*m*, C_6F_5, $^3J_{Fm\text{-}Fo/p}$ = 22.0 Hz, $^4J_{Fm\text{-}Fm}$ = 6.8 Hz); ring **c**, δ −131.25 (br s, 1F*o*, 1SC_6F_5), −132.58 (br s, 1F*o*′, 1SC_6F_5), −149.48 (t, 1F*p*, 1SC_6F_5, $^3J_{Fp\text{-}Fm}$ = 20.7 Hz), −159.38 (br s, 1F*m*, 1SC_6F_5), −160.31 (br s, 1F*m*′, 1SC_6F_5); ring **d**, δ −130.00 (m, 1F*o*, 1SC_6F_5), −130.81 (m, 1F*o*′, 1SC_6F_5), −150.66 (t, 1F*p*, 1SC_6F_5, $^3J_{Fp\text{-}Fm}$ = 20.7 Hz), −161.40 (m, 1F*m*, 1SC_6F_5), −161.64 (m, 1F*m*′, 1SC_6F_5).

Compound [Os(SC_6F_5)$_3$(SC_6F_4(SC_6F_5)-2)][25] (**c**) was isolated as green crystals (0.007 g, 4%).

[OsF(SC_6F_5)$_2$(SC_6F_4(SC_6F_5)-2)($P(C_6H_5)_3$)] (4a): green crystals (0.066 g, 33%). Anal. Calcd for $C_{42}H_{15}F_{20}OsPS_4$: C, 40.39; H, 1.21; S, 10.27. Found: C, 40.34; H, 1.40; S, 10.12. Mp: 184 °C, dec. IR (KBr, cm^{-1}): 1512(vs), 1494(vs), 1445(w), 1398(s), 1088(s), 979(s), 746(w), 693(w). FAB$^+$-MS {*m*/*z* (%) [fragment]}: 1231 (49) $[M^+ - F]$, 1051 (37) $[M^+ - (SC_6F_5)]$, 1032

(4) [$M^+ - F - (SC_6F_5)$], 871 (9) [$M^+ - (SC_6F_4(SC_6F_5))$], 770 (2) [$M^+ - F - (SC_6F_5) - (P(C_6H_5)_3)$], 603 (3) [$M^+ - F - (SC_6F_5) - (P(C_6H_5)_3) - (C_6F_5)$], 262 (100) $[P(C_6H_5)_3]^+$. ^{19}F NMR ($C_6D_5CD_3$, 80 °C), δ (ppm): ring **a**, δ −124.70 (m, 1F, C_6F_4), −129.87 (m, 1F, C_6F_4), −151.45 (m, 1F, C_6F_4), −153.93 (m, 1F, C_6F_4); ring **b**, δ −133.34 (d, 2F*o*, C_6F_5, $^3J_{Fo\text{-}Fm}$ = 21.8 Hz), −152.11 (t, 1F*p*, C_6F_5, $^3J_{Fp\text{-}Fm}$ = 20.7 Hz), −161.07 (m, 2F*m*, C_6F_5); rings **c**, δ −131.52 (br s, 4F*o*, 2SC_6F_5), −151.89 (br t, 2F*p*, 2SC_6F_5, $^3J_{Fp\text{-}Fm}$ = 19.6 Hz), −163.53 (br s, 4F*m*, 2SC_6F_5); F ligand, δ −192.59 (d, 1F*ax*, $^2J_{F\text{-}P}$ = 154 Hz). $^{31}P\{^1H\}$ NMR ($C_6D_5CD_3$, RT), δ (ppm): 0.22 (d, 1P, $P(C_6H_5)_3$).

[Os(SC_6F_5)$_2$(SC_6F_4(SC_6F_5)-2)(C_6H_5)] (4b): brown crystals (0.0085 g, 5%). Anal. Calcd for $C_{30}H_5F_{19}OsS_4$: C, 34.49; H, 0.48; S, 12.27. Found: C, 34.34; H, 0.60; S, 12.79. Mp: 220 °C, dec. IR (KBr, cm^{-1}): 1514(vs), 1506(vs), 1485(vs), 1460(s), 1392-(w), 1087(s), 978(s), 737(w). FAB^+-MS {*m*/*z* (%) [fragment]}: 1046 (1) M^+, 969 (3) [$M^+ - (C_6H_5)$], 847 (3) [$M^+ - (SC_6F_5)$], 770 (8) [$M^+ - (SC_6F_5) - (C_6H_5)$], 603 (2) [$M^+ - (SC_6F_5) - (C_6H_5) - (C_6F_5)$]. ^{19}F NMR ($C_6D_5CD_3$, RT), δ (ppm): ring **a**, δ −130.01 (ddd, 1F, C_6F_4, $^3J_{F\text{-}F}$ = 22.4 Hz, $^4J_{F\text{-}F}$ = 11.5 Hz, $^5J_{F\text{-}F}$ = 2.2 Hz), −132.28 (m, 1F, C_6F_4), −144.27 (td, 1F, C_6F_4, $^3J_{F\text{-}F}$ = 20.7 Hz, $^4J_{F\text{-}F}$ = 5.6 Hz), −152.11 (m, 1F, C_6F_4); ring **b**, δ −129.01 (m, 1F*o*, C_6F_5), −135.00 (d, 1F*o*′, C_6F_5, $^3J_{Fo\text{-}Fm}$ = 21.8 Hz), −143.48 (t, 1F*p*, C_6F_5, $^3J_{Fp\text{-}Fm}$ = 20.7 Hz), −156.61 (td, 1F*m*′, C_6F_5, $^3J_{Fm\text{-}Fo/p}$ = 22.0 Hz, $^4J_{Fm\text{-}Fm}$ = 6.8 Hz), −157.52 (td, 1F*m*, C_6F_5, $^3J_{Fm\text{-}Fo/p}$ = 22.0 Hz, $^4J_{Fm\text{-}Fm}$ = 5.6 Hz); ring **c**, δ −131.36 (br s, 1F*o*, 1SC_6F_5), −132.73 (br s, 1F*o*′, 1SC_6F_5), −149.99 (t, 1F*p*, 1SC_6F_5, $^3J_{Fp\text{-}Fm}$ = 20.7 Hz), −159.61 (br s, 1F*m*, 1SC_6F_5), −160.56 (br s, 1F*m*′, 1SC_6F_5); ring **d**, δ −130.21 (d, 1F*o*, 1SC_6F_5, $^3J_{Fo\text{-}Fm}$ = 23.3 Hz), −131.01 (d, 1F*o*′, 1SC_6F_5, $^3J_{Fo\text{-}Fm}$ = 24.4 Hz), −151.54 (t, 1F*p*, 1SC_6F_5, $^3J_{Fp\text{-}Fm}$ = 20.7 Hz), −161.95 (m, 1F*m*, 1SC_6F_5), −162.23 (m, 1F*m*′, 1SC_6F_5).

[Os(SC_6F_5)$_3$(SC_6F_4(SC_6F_5)-2)][25] (**c**) was isolated as green crystals (0.006 g, 3%).

[OsF(SC_6F_5)$_2$(SC_6F_4(SC_6F_5)-2)($P(C_6H_4CH_3$-4)$_3$)] (5a): green crystals (0.080 g, 40%). Anal. Calcd for $C_{45}H_{21}F_{20}OsPS_4$: C, 41.86; H, 1.64; S, 9.93. Found: C, 42.05; H, 1.83; S, 9.75. Mp: 150 °C, dec. IR (KBr, cm^{-1}): 1512(vs), 1494(vs), 1445(s), 1398(w), 1088(s), 978(vs), 806(w). FAB^+-MS {*m*/*z* (%) [fragment]}: 1273 (29) [$M^+ - F$], 1093 (24) [$M^+ - (SC_6F_5)$], 913 (7) [$M^+ - (SC_6F_4$-$(SC_6F_5))$], 304 (100) $[P(C_6H_4CH_3)_3]^+$. ^{19}F NMR ($C_6D_5CD_3$, 80 °C), δ (ppm): ring **a**, δ −124.81 (m, 1F, C_6F_4), −129.86 (m, 1F, C_6F_4), −151.66 (m, 1F, C_6F_4), −154.05 (m, 1F, C_6F_4); ring **b**, δ −133.32 (d, 2F*o*, C_6F_5, $^3J_{Fo\text{-}Fm}$ = 23.3 Hz), −152.33 (t, 1F*p*, C_6F_5, $^3J_{Fp\text{-}Fm}$ = 20.7 Hz), −161.18 (m, 2F*m*, C_6F_5); rings **c**, δ −131.58 (br s, 4F*o*, 2SC_6F_5), −152.09 (br m, 2F*p*, 2SC_6F_5), −163.64 (br s, 4F*m*, 2SC_6F_5); F ligand, δ −193.16 (d, 1F*ax*, $^2J_{F\text{-}P}$ = 148 Hz). $^{31}P\{^1H\}$ NMR ($C_6D_5CD_3$, RT), δ (ppm): −7.54 (d, 1P, $P(C_6H_4CH_3$-4)$_3$).

[Os(SC_6F_5)$_2$(SC_6F_4(SC_6F_5)-2)($C_6H_4CH_3$-4)] (5b): green crystals (0.020 g, 12%). Anal. Calcd for $C_{31}H_7F_{19}OsS_4$: C, 35.17; H, 0.67; S, 12.11. Found: C, 34.97; H, 0.85; S, 12.23. Mp: 184 °C, dec. IR (KBr, cm^{-1}): 1515(vs), 1497(vs), 1462(s), 1394(w), 1087(s), 979(s), 801(w). FAB^+-MS {*m*/*z* (%) [fragment]}: 1059 (9) [$M - H]^+$, 969 (36) [$M^+ - (C_6H_4CH_3)$], 861 (44) [$M^+ - (SC_6F_5)$], 770 (80) [$M^+ - (SC_6F_5) - (C_6H_4CH_3)$], 694 (7) [$M^+ - (SC_6F_5) - (C_6F_5)$], 662 (27) [$M^+ - 2(SC_6F_5)$], 603 (26) [$M^+ - (SC_6F_5) - (C_6H_4CH_3) - (C_6F_5)$], 436 (10) [$M^+ - (SC_6F_5) - (C_6H_4CH_3) - 2(C_6F_5)$], 436 (10) [$M^+ - (SC_6F_5) - (C_6H_4CH_3) - 2(C_6F_5)$], 404 (6) [$M^+ - 2(SC_6F_5) - (C_6H_4CH_3) - (C_6F_5)$]. ^{19}F NMR ($C_6D_5CD_3$, RT), δ (ppm): ring **a**, δ −130.05 (ddd, 1F, C_6F_4, $^3J_{F\text{-}F}$ = 22.3 Hz, $^4J_{F\text{-}F}$ = 10.9 Hz, $^5J_{F\text{-}F}$ = 2.6 Hz), −132.31 (m, 1F, C_6F_4), −144.39 (td, 1F, C_6F_4, $^3J_{F\text{-}F}$ = 21.2 Hz, $^4J_{F\text{-}F}$ = 6.8 Hz), −152.25 (m, 1F, C_6F_4, full integral = 2); ring **b**, δ −129.05 (m, 1F*o*, C_6F_5), −135.04 (d, 1F*o*′, C_6F_5, $^3J_{Fo\text{-}Fm}$ = 20.7 Hz), −143.56 (t, 1F*p*, C_6F_5, $^3J_{Fp\text{-}Fm}$ = 22.2 Hz), −156.65 (td, 1F*m*′, C_6F_5, $^3J_{Fm\text{-}Fo/p}$ = 22.6 Hz, $^4J_{Fm\text{-}Fm}$ = 6.8 Hz), −157.56 (td, 1F*m*, C_6F_5, $^3J_{Fm\text{-}Fo/p}$ = 22.0 Hz, $^4J_{Fm\text{-}Fm}$ = 7.2 Hz); ring **c**, δ −131.34 (br s, 1F*o*, 1SC_6F_5), −132.76 (br s, 1F*o*′, 1SC_6F_5), −150.11 (t, 1F*p*, 1SC_6F_5, $^3J_{Fp\text{-}Fm}$ = 20.7 Hz), −159.65 (br s, 1F*m*, 1SC_6F_5), −160.70 (br s, 1F*m*′, 1SC_6F_5); ring **d**, δ −129.88 (d, 1F*o*, 1SC_6F_5, $^3J_{Fo\text{-}Fm}$ = 24.8 Hz), −130.84 (d, 1F*o*′, 1SC_6F_5, $^3J_{Fo\text{-}Fm}$ = 26.0 Hz), −152.25 (m, 1F*p*, 1SC_6F_5, full integral = 2), −162.13 (m, 1F*m*, 1SC_6F_5), −162.35 (m, 1F*m*′, 1SC_6F_5).

[Os(SC_6F_5)$_2$($S_2C_6F_4$)($P(C_6H_4CH_3$-4)$_3$)] (5d): green crystals (0.0034 g, 2%). Anal. Calcd for $C_{39}H_{21}F_{14}OsPS_4$: C, 42.39; H, 1.92; S, 11.61. Found: C, 42.22; H, 1.85; S, 11.75. Mp: 220 °C, dec. IR (KBr, cm^{-1}): 1512(vs), 1494(vs), 1441(s), 1394(w), 1087(s), 979(s), 845(w). FAB^+-MS {*m*/*z* (%) [fragment]}: 1106 (38) M^+, 1087 (3) [$M^+ - F$], 1015 (2) [$M^+ - (C_6H_4CH_3)$], 939 (3) [$M^+ - (C_6F_5)$], 907 (12) [$M^+ - (SC_6F_5)$], 739 (10) [$M^+ - (SC_6F_5) - H - (C_6F_5)$], 727 (2) [$M^+ - (C_6F_5) - (S_2C_6F_4)$], 615 (3) [$M^+ - 2(SC_6F_5) - (C_6H_4CH_3) - 2H$].

[OsF(SC_6F_5)$_2$(SC_6F_4(SC_6F_5)-2)($P(C_6H_4OCH_3$-4)$_3$)] (6a): green powder (0.046 g, 23%). Anal. Calcd for $C_{45}H_{21}F_{20}O_3OsPS_4$: C, 40.36; H, 1.58; S, 9.58. Found: C, 40.42; H, 1.72; S, 9.51. Mp: 175 °C, dec. IR (KBr, cm^{-1}): 1514(vs), 1498(vs), 1445(s), 1398(w), 1258(s), 1088(s), 980(s), 801(w). FAB^+-MS {*m*/*z* (%) [fragment]}: 1321 (18) [$M^+ - F$], 1154 (1) [$M^+ - F - (C_6F_5)$], 1141 (14) [$M^+ - (SC_6F_5)$], 1122 (4) [$M^+ - F - (SC_6F_5)$], 961 (3) [$M^+ - (SC_6F_4(SC_6F_5))$], 770 (1) [$M^+ - F - (SC_6F_5) - (P(C_6H_4OCH_3)_3)$], 603 (2) [$M^+ - F - (SC_6F_5) - (P(C_6H_4OCH_3)_3) - (C_6F_5)$], 352 (100) $[P(C_6H_4$-$OCH_3)_3]^+$. ^{19}F NMR ($C_6D_5CD_3$, 80 °C), δ (ppm): ring **a**, δ −124.76 (m, 1F, C_6F_4), −129.72 (m, 1F, C_6F_4), −151.61 (m, 1F, C_6F_4), −153.93 (m, 1F, C_6F_4); ring **b**, δ −133.22 (d, 2F*o*, C_6F_5, $^3J_{Fo\text{-}Fm}$ = 21.8 Hz), −152.23 (t, 1F*p*, C_6F_5, $^3J_{Fp\text{-}Fm}$ = 20.7 Hz), −161.05 (m, 2F*m*, C_6F_5); rings **c**, δ −131.45 (br s, 4F*o*, 2SC_6F_5), −152.02 (br t, 2F*p*, 2SC_6F_5, $^3J_{Fp\text{-}Fm}$ = 18.1 Hz), −163.50 (br s, 4F*m*, 2SC_6F_5); F ligand, δ −193.62 (d, 1F*ax*, $^2J_{F\text{-}P}$ = 156 Hz). $^{31}P\{^1H\}$ NMR ($C_6D_5CD_3$, RT), δ (ppm): −5.10 (d, 1P, $P(C_6H_4OCH_3$-4)$_3$).

[Os(SC_6F_5)$_2$(SC_6F_4(SC_6F_5)-2)($C_6H_4OCH_3$-4)] (6b): green crystals (0.015 g, 9%). Anal. Calcd for $C_{31}H_7F_{19}OOsS_4$: C, 34.64; H, 0.66; S, 11.93. Found: C, 34.72; H, 0.80; S, 11.82. Mp: 180 °C, dec. IR (KBr, cm^{-1}): 1513(vs), 1499(vs), 1463(s), 1393(w), 1086(s), 980(s), 847(w). FAB^+-MS {*m*/*z* (%) [fragment]}: 1076 (17) $[M]^+$, 969 (42) [$M^+ - (C_6H_4OCH_3)$], 877 (38) [$M^+ - (SC_6F_5)$], 770 (56) [$M^+ - (SC_6F_5) - (C_6H_4OCH_3)$], 678 (21) [$M^+ - 2(SC_6F_5)$], 603 (20) [$M^+ - (SC_6F_5) - (C_6H_4OCH_3) - (C_6F_5)$], 436 (6) [$M^+ - (SC_6F_5) - (C_6H_4OCH_3) - 2(C_6F_5)$]. ^{19}F NMR ($C_6D_5CD_3$, RT), δ (ppm): ring **a**, δ −130.16 (ddd, 1F, C_6F_4, $^3J_{F\text{-}F}$ = 24.8 Hz, $^4J_{F\text{-}F}$ = 11.5 Hz, $^5J_{F\text{-}F}$ = 4.1 Hz), −132.31 (m, 1F, C_6F_4), −144.42 (td, 1F, C_6F_4, $^3J_{F\text{-}F}$ = 21.2 Hz, $^4J_{F\text{-}F}$ = 6.8 Hz), −152.26 (m, 1F, C_6F_4); ring **b**, δ −129.17 (m, 1F*o*, C_6F_5), −135.08 (d, 1F*o*, C_6F_5, $^3J_{Fo\text{-}Fm}$ = 23.3 Hz), −143.67 (tt, 1F*p*, C_6F_5, $^3J_{Fp\text{-}Fm}$ = 20.7 Hz, $^4J_{Fp\text{-}Fo}$ = 4.1 Hz), −156.69 (td, 1F*m*′, C_6F_5, $^3J_{Fm\text{-}Fo/p}$ = 22.8 Hz, $^4J_{Fm\text{-}Fm}$ = 8.3 Hz), −157.57 (td, 1F*m*, C_6F_5, $^3J_{Fm\text{-}Fo/p}$ = 22.2 Hz, $^4J_{Fm\text{-}Fm}$ = 6.8 Hz); ring **c**, δ −131.47 (br s, 1F*o*, 1SC_6F_5), −132.71 (br s, 1F*o*′, 1SC_6F_5), −150.13 (t, 1F*p*, 1SC_6F_5, $^3J_{Fp\text{-}Fm}$ = 20.7 Hz), −159.70 (br s, 1F*m*, 1SC_6F_5), −160.66 (br s, 1F*m*′, 1SC_6F_5)); ring **d**, δ −129.83 (d, 1F*o*, 1SC_6F_5, $^3J_{Fo\text{-}Fm}$ = 24.8 Hz), −130.75 (d, 1F*o*, 1SC_6F_5, $^3J_{Fo\text{-}Fm}$ = 23.3 Hz), −152.04 (t, 1F*p*, 1SC_6F_5, $^3J_{Fp\text{-}Fm}$ = 20.7 Hz), −162.14 (m, 1F*m*, 1SC_6F_5), −162.37 (m, 1F*m*′, 1SC_6F_5).

[Os(SC_6F_5)$_3$(SC_6F_4(SC_6F_5)-2)][25] (**c**) was isolated as green crystals (0.005 g, 3%).

Crystallography. Air-stable single crystals of complexes **2b**−**6b** and **5d** were obtained by slow evaporation of their air-stable solutions (hexane−CH_2Cl_2, 4:1). However, crystals of **4a** and **5a** were obtained from their solutions (hexane−CH_2Cl_2, 1:9) under argon atmospheres, because of their air sensitivity in solution. A green mixture of **2a** and **2e** was dissolved in hexane−CH_2Cl_2 (1:9) and kept under Ar atmosphere. After a few hours the solution turned purple with decomposition of **2a**, and over time, a dark green crystal of **2e** deposited.

Table 1. X-ray Parameters

	4a	**5a**	**2b**	**3b**
chem formula	$C_{42}H_{15}F_{20}OsPS_4$	$C_{45}H_{21}F_{20}OsPS_4 \cdot 0.5(H_2O)$	$C_{30}H_4ClF_{19}OsS_4$	$C_{30}H_4F_{20}OsS_4$
fw	1248.95	1300.04	1079.22	1062.77
space group	$P\bar{1}$	$P\bar{1}$	$P\bar{1}$	$P\bar{1}$
a/Å	11.4570(11)	11.6506(13)	10.7595(18)	10.7540(12)
b/Å	12.0914(11)	12.6198(14)	12.3939(12)	12.3279(11)
c/Å	18.4994(16)	18.777(2)	13.8046(16)	13.1539(13)
α/deg	84.886(5)	77.420(8)	72.201(6)	73.671(7)
β/deg	73.213(6)	72.116(8)	79.379(11)	80.942(9)
γ/deg	64.074(6)	67.338(9)	82.299(10)	83.05(1)
V/Å^3	2204.6(3)	2408.9(5)	1716.8(4)	1647.2(3)
Z	2	2	2	2
μ/mm^{-1}	3.235	2.965	4.163	4.262
R indices [$I > 2\sigma(I)$][a]	0.039, 0.062	0.043, 0.092	0.034, 0.083	0.070, 0.197
R indices (all data) [a]	0.064, 0.068	0.061, 0.099	0.043, 0.090	0.081, 0.205
D_{calc}/g cm^{-3}	1.881	1.792	2.088	2.143
data/params	6088/613	8365/658	7745/496	5690/496
S[a]	1.047	1.015	1.017	1.120

	4b	**5b**	**6b**	**5d**	**2e**
chem formula	$C_{30}H_5F_{19}OsS_4$	$C_{31}H_7F_{19}OsS_4$	$C_{31}H_7F_{19}OOsS_4$	$C_{39}H_{21}F_{14}OsPS_4$	$C_{36}H_{12}Cl_3F_{16}OsPS_3 \cdot 1.38(CH_2Cl_2)$
fw	1044.78	1058.81	1074.81	1104.97	1289.35
space group	$P\bar{1}$	$P\bar{1}$	$P\bar{1}$	$P\bar{1}$	$R\bar{3}$
a/Å	10.7829(13)	10.5552(10)	11.2820(7)	10.648(2)	15.3769 (13)
b/Å	12.2538(13)	12.3092(13)	12.5292(8)	14.992(2)	15.3769 (13)
c/Å	12.7859(15)	13.6336(11)	12.6534(7)	15.431(3)	34.068 (4)
α/deg	74.697(7)	87.486(8)	80.587(5)	69.348(10)	90
β/deg	82.010(10)	76.577(4)	78.904(4)	85.700(13)	90
γ/deg	83.771(9)	82.634(10)	75.411(6)	74.435(12)	120
V/Å^3	1609.1(3)	1708.6(3)	1686.07(18)	2219.8(7)	6976.2 (11)
Z	2	2	2	2	6
μ/mm^{-1}	4.357	4.105	4.164	3.182	3.335
R indices [$I > 2\sigma(I)$][a]	0.026, 0.061	0.034, 0.081	0.030, 0.067	0.047, 0.102	0.052, 0.112
R indices (all data) [a]	0.032, 0.063	0.043, 0.086	0.038, 0.070	0.076, 0.114	0.092, 0.124
D_{calc}/g cm^{-3}	2.156	2.058	2.117	1.653	1.841
data/params	9286/488	8867/497	8897/506	5978/535	2727/181
S[a]	1.040	1.062	1.053	1.013	1.011

[a] $R_1 = [\sum||F_o| - |F_c||]/[\sum|F_o|]$, $wR_2 = [\sum w(F_o^2 - F_c^2)^2/\sum w(F_o^2)^2]^{1/2}$, $S = [\sum w(F_o^2 - F_c^2)^2/(\text{data} - \text{params})]^{1/2}$.

Pertinent crystal data and other crystallographic parameters are listed in Table 1. Diffraction data were collected at room temperature (294−298 K) using a Bruker P4 diffractometer equipped with Mo Kα radiation ($\lambda = 0.71073$ Å), using the standard procedure,[52] and raw data were corrected for absorption effects using suitable Ψ-scan data.[53] In all cases, the Os site may be found by interpreting a Patterson map, and the structure of the complex was completed by analyzing difference maps. Final refinements were carried out[54] without restraints nor constraints for non-H atoms. H atoms were placed in idealized positions and refined as riding on their carrier C atoms. In the case of **5a**, the crystal was found to be a hemihydrate, and the water molecule geometry was regularized through soft restraints, O−H = 0.85(1) Å and H···H = 1.34(2) Å. The somewhat disappointing refinements for **3b** and **5d** (R_1 = 7% and 5%, respectively) are a consequence of the crystal habits: these complexes crystallize as very thin plates with a thickness of ca. 40 μm, which makes the correction for absorption difficult to apply. For both complexes **4a** and **5d**, data resolution was also limited to 0.91 Å ($2\theta_{max}$ = 46° for Mo Kα radiation) since crystals are poorly diffracting samples. In the case of **2e**, molecules are packed in the crystal in such a way that large void spaces are present, representing 18.8% of the unit cell volume. Since the shape of the voids does not match the geometry of *n*-hexane, they were assumed to be filled by disordered CH_2Cl_2 molecules. The contribution of the disordered solvent to the structure factors was estimated using the SQUEEZE procedure implemented in PLATON.[55] A total of 347 electrons per unit cell were recovered, interpreted as 8.26 solvent molecules per unit cell, i.e., 1.38 solvent molecules per osmium complex ($Z = 6$). In the thiolate benzene ring, the C10−C11 bond length was restrained to 1.37(1) Å; otherwise this bond length converged to a too small distance of ca. 1.30 Å. Complete geometric parameters may be consulted from the archived CIF file, and diffraction data are available on request from the authors.

Acknowledgment. We gratefully acknowledge CONACYT (27915E), VIEP (ARCS-NAT-09-G), and PROMEP for financial support. S.B. acknowledges BUAP for the use of diffraction facilities.

Supporting Information Available: X-ray crystallographic files, in CIF format, for the structures of compounds **4a**, **5a**, **2b**−**6b**, **5d**, and **2e** are available free of charge via the Internet at http://pubs.acs.org.

(52) *XSCAnS* (*release 2.21*) *Users Manual*; Siemens Analytical X-ray Instruments Inc.: Madison, WI, 1996.

(53) North, A. C. T.; Phillips, D. C.; Mathews, F. S. *Acta Crystallogr.* **1968**, *A24*, 351–359.

(54) Sheldrick, G. M. *Acta Crystallogr.* **2008**, *A64*, 112–122.

(55) Spek, A. L. *J. Appl. Crystallogr.* **2003**, *36*, 7–13.